Hydrological Processes

WILEY

RESEARCH ARTICLE OPEN ACCESS

Multi-Year Evapotranspiration and Energy Dynamics of a Reclaimed Fen in the Athabasca Oil Sands Region

Daniel Amaro Medina[1] | M. Graham Clark[2] | Sean K. Carey[1]

[1]School of Earth, Environment & Society, McMaster University, Hamilton, Canada | [2]Department of Earth and Environmental Sciences, St. Francis Xavier University, Antigonish, Canada

Correspondence: Daniel Amaro Medina (amaromed@mcmaster.ca)

Received: 9 April 2025 | **Revised:** 3 July 2025 | **Accepted:** 6 August 2025

Funding: This work was supported by the Syncrude.

Keywords: Athabasca Oil Sands region | constructed fen | eddy covariance | evapotranspiration | reclamation | *Typha latifolia*

ABSTRACT

Surface mining in the Athabasca Oil Sands Region (AOSR) of western Canada disrupts natural landscapes and permanently alters their hydrological functions. Wetlands cover ~55% of the region, primarily fen peatlands, and although provincial regulations require companies to restore disturbed ecosystems to a functional state, fens remain difficult to construct due to their complex hydrology and dependence on water exchange with surrounding uplands. Evapotranspiration (ET), a key component of the water balance, is particularly important in the sub-humid AOSR, where increasing reclamation activity demands accurate quantification of vertical water loss, as it influences ecohydrological feedbacks and long-term wetland sustainability. This study evaluates ET and energy dynamics in a constructed fen, built atop ~80 m deposit of composite tailings and capped with 10 m of tailings sand, using eddy covariance (EC) measurements and vegetation surveys conducted across five non-consecutive years between 2015 and 2023. Mean ET from April 1 to October 31 was 250 ± 49.9 mm, aligning with values from natural and constructed boreal peatlands. On average, ET was 15% higher in warmer and drier years. While intra-annual ET variability was mainly influenced by vapour pressure deficit and net radiation, a long-term decline in ET coincided with *Typha latifolia* expansion, whose canopy reduced water loss by sheltering the open water. Flux partitioning revealed that transpiration exceeded evaporation by up to 70%, highlighting the role of *Typha* in reducing energy input and limiting turbulent mixing over the ponded water surface. Despite declining ET, latent heat flux remained the dominant component of the energy balance, suggesting functional similarity to natural fens. With rainfall exceeding ET in 80% of the years, the study site did not experience any prolonged drought periods. These findings enhance understanding of surface-atmosphere interactions and inform wetland reclamation strategies, particularly the role of vegetation change.

1 | Introduction

Boreal wetlands are critical ecosystems that play a vital role in carbon sequestration, greenhouse gas regulation, water management, and pollutant filtration and retention (Webster et al. 2015). In the Athabasca Oil Sands Region of Alberta, which spans approximately 90 000 km^2, ~4750 km^2 is deemed surface-mineable, and approximately 1055 km^2 is already disturbed, significantly altering the hydrological functions of surrounding wetlands (Volik et al. 2020; Popović et al. 2025). Provincial legislation under the Environmental Protection and Enhancement Act mandates that mining companies restore disturbed sites to an equivalent land capability similar to pre-disturbance conditions. However, due to differences

This is an open access article under the terms of the Creative Commons Attribution License, which permits use, distribution and reproduction in any medium, provided the original work is properly cited.

© 2025 The Author(s). *Hydrological Processes* published by John Wiley & Sons Ltd.

between mine materials and natural substrates, reconstructed landscapes physically differ from their original state, often resulting in hybrid or novel ecosystems (Nwaishi et al. 2015; AEP 2018).

The undisturbed landscape of the AOSR consists of a mosaic of boreal forests (~25%) and wetlands (~55%), with fen peatlands comprising the largest portion (Rooney et al. 2012; Volik et al. 2020). While past research has largely focused on forest reestablishment (Carey 2008; Macdonald et al. 2012; Huang et al. 2015; Strilesky et al. 2017; Amaro Medina and Carey 2024), recent efforts have shifted toward peatland construction due to the critical ecological functions of these ecosystems (Daly et al. 2012; Wytrykush et al. 2012; Ketcheson et al. 2016, 2017; Nicholls et al. 2016; Scarlett et al. 2017; Biagi et al. 2021; Clark et al. 2022; Popović et al. 2022, 2023). Fen construction is particularly challenging due to the complex hydrology, geomorphology, and extended timescales required for natural peatland formation. Nonetheless, successful peatland reestablishment is feasible if the constructed ecosystem meets the necessary geological and hydrological conditions (Devito et al. 2012; Oswald and Carey 2016).

The success of reclamation efforts depends on reestablishing hydrologically connected landscapes (i.e., hydrologic units), particularly for peatlands, which require consistent water availability (Devito et al. 2012). This is challenging in the sub-humid AOSR, where annual precipitation is typically lower than evapotranspiration (ET), leading to frequent water deficits (Brown et al. 2010; Popović et al. 2022). Apart from their ecological functions, wetlands play a crucial role in constructed landscapes due to their hydrological connectivity with surrounding uplands, which is essential for distributing water to downstream fluvial systems. This two-way wetland–upland interaction is particularly important for sustaining surface–groundwater exchange and maintaining the hydrological integrity of the landscape (Volik et al. 2024). Therefore, understanding the environmental and climatic controls on the hydrology of constructed peatlands is crucial for ensuring their long-term sustainability and developing suitable water management strategies. Despite projections of approximately a 10% increase in total precipitation by 2050 in the AOSR, air temperature is expected to rise more substantially (3.3°C, CMIP6-SSP3-7.0; ClimateData.ca 2025). This warming may lead to drier conditions and reduced water availability (Ireson et al. 2015; Thompson et al. 2017), highlighting the need for long-term assessments of ecosystem function and response to environmental change.

ET is a key component of the regional water balance and understanding the biotic and abiotic factors that control its variability is critical for refining reclamation strategies and minimising water losses in constructed peatlands. Previous studies in the AOSR have examined short-term (~3 years) changes in constructed fens' hydrology and hydrochemistry (Nicholls et al. 2016; Oswald and Carey 2016; Spennato et al. 2018; Biagi et al. 2019; Biagi and Carey 2020), vegetation dynamics (Scarlett et al. 2017; Vitt et al. 2020), and carbon cycling (Clark et al. 2019). However, long-term investigations of surface-atmosphere exchanges in reclaimed peatlands remain limited, with only a few recent studies encapsulating surface energy fluxes behaviour in these ecosystems (Popović et al. 2023, 2025).

Research on boreal peatlands indicates that ET is influenced primarily by climate conditions, vegetation cover, and water table fluctuations (Wu et al. 2010; Moore et al. 2013; Runkle et al. 2014; Helbig et al. 2020; Biagi et al. 2021). However, the relationship between water table depth and ET remains uncertain due to weak correlations observed in some peatland ecosystems (Lafleur et al. 2005; Faubert and Carey 2014). Among climatic drivers, vapour pressure deficit and net radiation are considered dominant, with the latter typically exerting a stronger influence on ET rates (Petrone et al. 2007; Nicholls et al. 2016; Volik, Kessel, et al. 2021). In the AOSR, research on wetland ET has primarily focused on native fen vegetation (e.g., Scarlett et al. 2017). Specifically, most studies examined changes in plant communities solely in relation to salinity and sodium concentration effects (Vitt et al. 2016, 2020; House et al. 2022). However, less attention has been given to emergent aquatic species uncommon in fens, such as *Typha latifolia*, whose effects on microclimate and ET remain poorly understood. Most research on *Typha* was conducted in marshes (Goulden et al. 2007) or within broader restoration studies (Bourgeois et al. 2012; Graham et al. 2022). While some studies acknowledge *Typha's* adaptability to constructed peatlands (Mollard et al. 2013), concerns persist regarding its potential to inhibit peat formation and reduce plant diversity, thereby impeding reclamation success (Popović et al. 2023).

Given the complexity and heterogeneity of peatlands, identifying the vegetation controls on ET is a challenging task. A valuable approach to addressing this challenge is partitioning ET into its components—evaporation (E) and transpiration (T). Accurate ET partitioning enhances the understanding of water and energy exchanges between the ecosystem and atmosphere (Xu et al. 2021), which is essential for developing effective strategies to maintain water availability critical for peatland functionality. While ET partitioning studies have been conducted in forests, shrublands, and grasslands (Hu et al. 2009; Cavanaugh et al. 2011; Paul-Limoges et al. 2020), research specifically quantifying evaporation and transpiration in peatlands remains scarce.

Considering the critical role of ET in the boreal water budget and the widespread presence of *Typha* in reconstructed peatlands, this study aims to evaluate ET responses to environmental variations in a reclaimed fen over five non-consecutive years (2015, 2017, 2019, 2021, and 2023) within a 10-year period. We hypothesise that both intraseasonal and interannual variability in climate conditions, along with changes in vegetation cover in the constructed fen, contribute to variations in ET rates, leading to measurable differences over the observation period. To test this hypothesis, we use the eddy covariance (EC) technique and vegetation survey data to address the following key objectives: (1) identify the primary environmental factors regulating growing season ET and its components in the fen ecosystem; (2) assess inter-annual ET variability in response to shifts in dominant plant communities and regional climate conditions; and (3) evaluate the hydrological function of the study fen relative to natural and reconstructed ecosystems. These insights are essential for assessing the effectiveness of current peatland

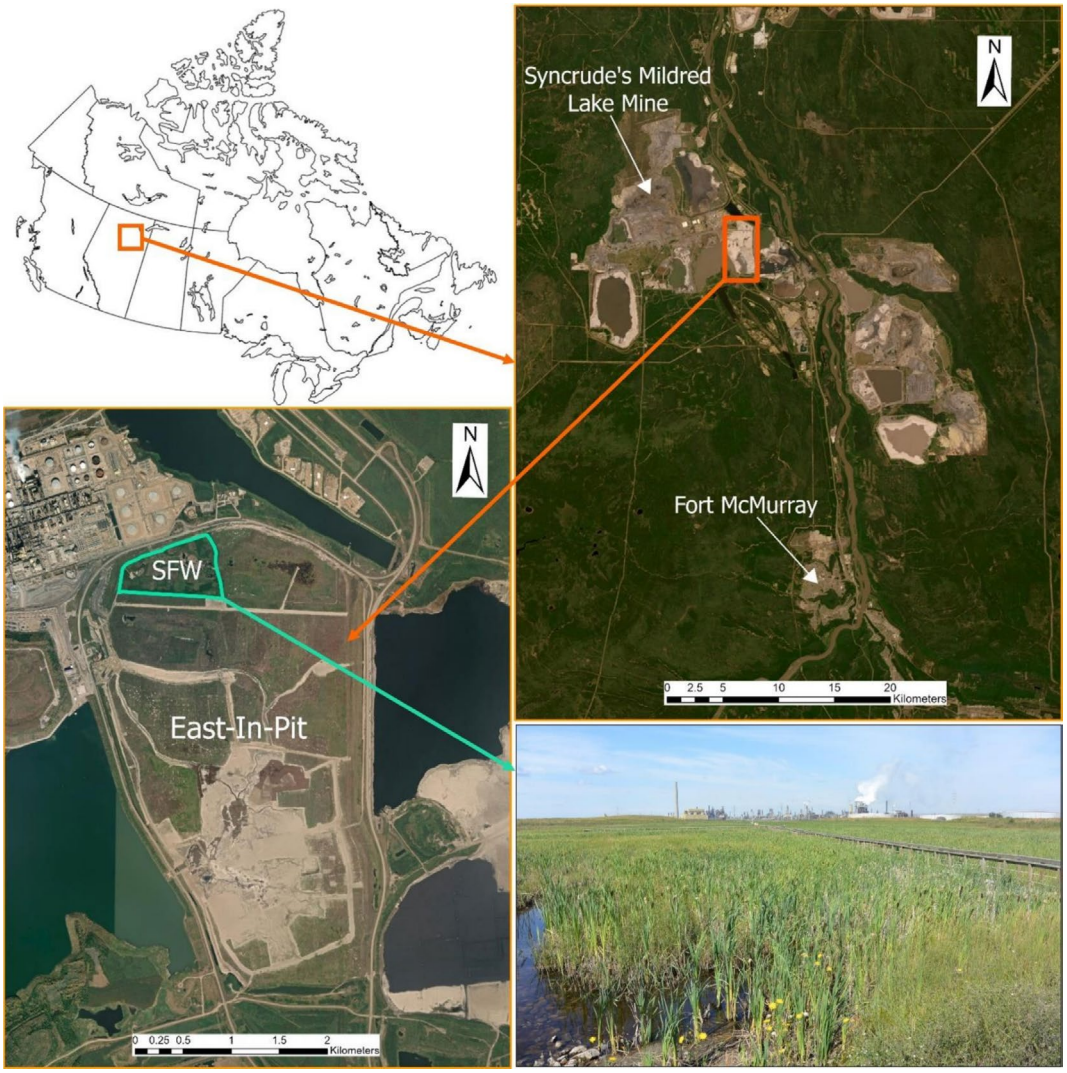


FIGURE 1 | Map of Canada with the location of the AOSR (top left); Fort McMurray and surrounding mining sites (right–orange square indicates the location of the study area); East-in-Pit and Sandhill Fen Watershed location (bottom left); view of Sandhill Fen (bottom right).

reclamation practices and ensuring the long-term sustainability of these ecosystems.

2 | Materials and Methods

2.1 | Study Area

The study site, Sandhill Fen, is one of two pilot projects established to monitor the development of peatland ecosystems in the post-mining landscape of the Athabasca Oil Sands Region and is located approximately 40 km north of Fort McMurray in northeastern Alberta, Canada (Figure 1). It is a constructed fen within the Sandhill Fen Watershed (SFW), situated in the northwestern corner of Mildred Lake Mine, within the East-In-Pit (EIP) soft tailings deposit, covering an area of 0.52 km^2. EIP was mined between 1977 and 1999 (Wytrykush et al. 2012). The mined-out pit was then infilled with a 60–100 m layer of pure tailings sand (the residual sand left after bitumen is extracted from the oil sands ore) and composite tailings (a mixture of fluid fine tailings and sand tailings) between 1999 and 2008. The SFW was constructed over 4 years (2009–2012) on top of the filled pit and a 10 m sand structural cap, which was engineered to form the topography of the newly constructed watershed (Clark et al. 2019). The primary design elements of the Sandhill Fen Watershed encompass constructed upland hills (i.e., hummocks), vegetated swales, a fen wetland, a freshwater storage pond, an under-drain system for the fen, and two perched fen wetlands (Figure 2). The main function of the hummocks is to provide water to the lowlands and minimise the salinization of vegetation roots. The primary water sources for SFW are precipitation inputs and groundwater recharge, while fen outflows are controlled by pumping operations (Nicholls et al. 2016; Biagi et al. 2021). The pumps were initially intended to maintain wetness and control salinity to support vegetation growth in the developing ecosystem (Biagi et al. 2019). Currently, with inflow halted, they are primarily used to regulate outflow and prevent water stagnation and excessively high water levels in the fen.

2.2 | SFW Instrumentation Network

Sandhill Fen Watershed is one of the most extensively studied reclamation projects in the AOSR and has a large instrumentation

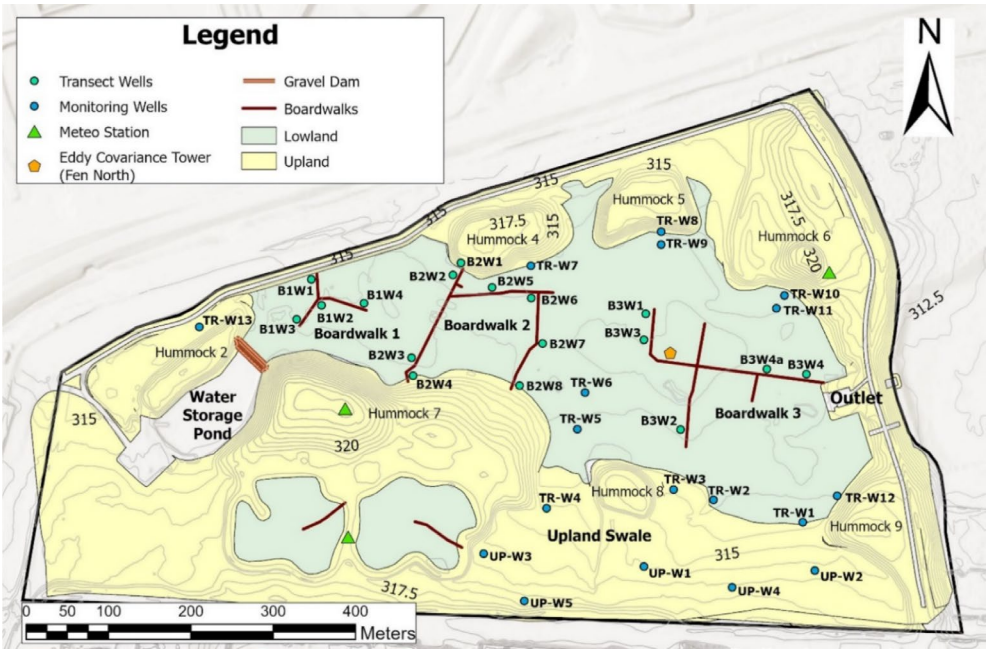


FIGURE 2 | Instrumentation network of the SFW; lowlands are represented in light green and uplands—in yellow.

network (Figure 2). To collect data on climate parameters, three meteorological towers were installed across the SFW to measure air temperature, wind speed, and direction, relative humidity, as well as shortwave and longwave radiation (Biagi et al. 2021). In addition, there is an EC tower located on Boardwalk 3 near the center of the wetland. The tower is equipped with a three-dimensional sonic anemometer (Campbell Scientific, model CSAT-3) measuring wind speed and direction, an enclosed path infrared gas analyser (LI-COR Biosciences, model LI-7200) measuring H_2O and CO_2 mixing ratios, and a CNR4 net radiometer. The instrumentation is mounted 2.9 m above the fen's surface. Further details on SFW's well network and other monitoring equipment can be found in Biagi et al. (2021).

2.3 | Data Collection and Processing

2.3.1 | EC and Micrometeorology

Half-hourly fluxes were calculated using EddyPro software (v7.0.9, LI-COR Inc., USA) and processed following standard procedures for EC data (Vickers and Mahrt 1997; Moncrieff et al. 2005; Mauder et al. 2013). Latent (LE) and sensible (H) heat fluxes were gap-filled using an Artificial Neural Network (ANN) algorithm, as described by Clark et al. (2019). Environmental variables that influence these fluxes—air temperature (T_a), net radiation (R_n), vapour pressure deficit (VPD), and wind speed (U), along with seasonal dummy vectors (sine and cosine)—were selected as inputs to the ANN due to their reliable data availability (99.6%–99.9%). Both observed and gap-filled data are shown in Figure S1.

In this study, T_a and VPD were averaged from the three Syncrude weather stations located on the SFW hummocks (labelled as Meteo Station in Figure 2). Net radiation and heat fluxes were converted from watts per square meter ($W\,m^{-2}$) to megajoules per square meter per day ($MJ\,m^{-2}\,d^{-1}$) to enable compatibility with subsequent analyses conducted at a daily temporal resolution.

2.3.2 | Surface-Atmosphere Interaction Parameters

Surface-atmosphere interaction parameters were derived from half-hourly flux data and included aerodynamic conductance (g_a), surface conductance (g_s), and the decoupling factor (Ω).

Aerodynamic conductance represents the efficiency of an ecosystem in transferring latent and sensible heat to the atmosphere through turbulent mixing (Peichl et al. 2013). It was calculated as the inverse of aerodynamic resistance and converted from $m\,s^{-1}$ to $mm\,s^{-1}$ (Humphreys et al. 2006; see SI, Equation S1).

Surface conductance, expressed in $m\,s^{-1}$ and converted to $mm\,s^{-1}$, regulates the transfer of water vapour from the land surface to the atmosphere, including through plant stomata, soil, and wet surfaces (Schulze et al. 1995), and derived by rearranging the Penman-Monteith equation (Helbig et al. 2020; see SI, Equation S2).

To evaluate the degree of interaction between the atmosphere and fen vegetation, we estimated a vegetation-atmosphere decoupling factor (Jarvis and McNaughton 1986; see SI, Equation S3). An Ω value near 0 indicates a well-coupled ecosystem, where ET is primarily regulated by stomatal control over transpiration and influenced by VPD. In contrast, when Ω approaches 1, the system is uncoupled, and ET is predominantly determined by the amount of available energy (Popović et al. 2023).

2.3.3 | Actual and Reference ET

Actual evapotranspiration (ET_a) was derived from the latent heat flux using the following expression (Allen et al. 1998):

$$ET_a = \frac{LE * D}{L_v \rho_w} \quad (1)$$

where LE is the latent heat flux ($W\,m^{-2}$), D is the time conversion factor (3600 for hourly time steps and 86 400 for daily time steps), ρ_w is the water density ($997\,kg\,m^{-3}$), and L_v is the latent heat of vaporisation ($J\,kg^{-1}$) expressed as (Harder and Pomeroy 2013):

$$L_v = 1000 * (2501 - 2.36T_a) \quad (2)$$

The reference evapotranspiration rate (ET_o), expressed in millimetres per day (mm d^{-1}), was calculated using the Penman-Monteith combination equation as recommended by the Food and Agriculture Organisation of the United Nations (Allen et al. 1998):

$$ET_o = \frac{0.408s(R_n - G) + \gamma \frac{900}{T_a + 273} u_2 (e_s - e_a)}{s + \gamma(1 + 0.34u_2)} \quad (3)$$

where s is the change in saturation pressure with temperature ($kPa\,°C^{-1}$), R_n is the net radiation flux ($MJ\,m^{-2}\,d^{-1}$), G is the ground heat flux ($MJ\,m^{-2}\,d^{-1}$), γ is the psychrometric constant ($kPa\,°C^{-1}$), T_a is the air temperature (°C), u_2 is the wind speed at 2 m above the ground ($m\,s^{-1}$), e_s is the saturated vapour pressure (kPa), e_a is the actual vapour pressure (kPa). For daily calculations, G was assumed to be zero (Gavilán et al. 2007), and u_2 was estimated by adjusting the actual measured wind speed at the observation tower using the following equation (Zotarelli et al. 2010):

$$u_2 = u_h \frac{4.87}{\ln(67.8h - 5.42)} \quad (4)$$

where u_z is the measured wind speed z m above the ground surface ($m\,s^{-1}$) and h is the measurement height (m).

2.3.4 | ET Partitioning

To partition ET into its components, evaporation (E) and plant transpiration (T), we used an open-source Python algorithm developed by Zahn and Bou-Zeid (2024). Of the five partitioning methods, the conditional EC (CEC) method was most applicable for this study due to its established reliability (Gao et al. 2023; Wang et al. 2024), independence from supplementary data (e.g., water-use efficiency, gross primary production), and ability to directly partition fluxes using continuous high-frequency EC measurements (Zahn et al. 2022, 2024).

CEC is based on the assumed similarity between water vapour and carbon dioxide fluxes, with key assumptions including (Zahn and Bou-Zeid 2024): (1) The EC system height (z_{EC}) should be close to the mean canopy height (z_c) (ideally, $z_{EC}/z_c < 3$) to capture both soil and vegetation fluxes accurately; (2) soil (evaporation, respiration) and vegetation (transpiration, photosynthesis) fluxes must be non-negligible; and (3) the correlation or anticorrelation between water vapour and carbon dioxide fluxes should not be perfect. Further details on the CEC method can be found in the SI (Section S2) and Zahn et al. (2022).

To satisfy one of the open-source algorithm requirements ($T_a > 0$) and to capture peak vegetation activity at the fen, we limited our analysis of high-frequency EC data to the growing season (June 1–August 31). This period was selected to assess the influence of environmental factors and vegetation shifts on summer ET, E, and T. Data processing followed the protocol outlined in the open-source script, with half-hourly estimates of E and T components ($W\,m^{-2}$) aggregated to a daily timescale (mm d^{-1}), yielding 92 observations per year. To account for intra-daily variability, both daytime and nighttime fluxes were included, with nighttime defined as periods when downwelling shortwave radiation (R_{Sdn}) was less than $10\,W\,m^{-2}$.

2.3.5 | Vegetation Conditions

Our study examined the distribution and temporal shifts of key dominant species within the Sandhill Fen, specifically *Typha latifolia* (broad-leaved cattail) and *Carex aquatilis* (water sedge). The data were obtained from House et al. (2022), who conducted systematic repeated vegetation surveys using a grid of approximately 90 permanent plots in 2015, 2017, 2019, and 2021.

In the 16 plots closest to the tower, the abundance of *Typha latifolia* increased from 19% in 2015 to 63% in 2021, notably expanding into areas previously dominated by *Carex* (Table 3 and Figure 3). Conversely, the abundance of *Carex aquatilis* declined in the central parts of the fen, decreasing from 32% in 2015 to 13% in 2021; it was displaced toward the fen's periphery (Table 3 and Figure 4).

Further details on the potential drivers of the shifts in dominant vegetation species, the abundance of other plant species, and associated changes in water chemistry within the fen are available in House et al. (2022).

2.4 | Data Analysis

For the analysis, we selected data from April 1 to October 31 (hereafter referred to as the 'study period') for each odd year between 2015 and 2023. Specifically, the years 2015, 2017, 2019 and 2021 were chosen due to the availability of dominant plant species data from vegetation surveys conducted in the SFW during those periods (Figures 3 and 4). The year 2023 was included as an additional year of observation to assess ongoing changes in the fen ecosystem over time.

To address discrepancies in measurement intervals among variables, all data were standardised to a daily scale and extracted for the study period, resulting in 214 observation points per year. Additionally, the study periods were categorised based on deviations from the 30-year climate normal for Fort McMurray Airport. The categories include 'warm' and 'cool' for temperature conditions and 'dry' and 'wet' for precipitation conditions. Warm and cool periods were defined by air temperatures exceeding the 75th percentile and falling below the 25th percentile, respectively. Similarly, wet and dry periods were determined by total precipitation outside these quartile thresholds.

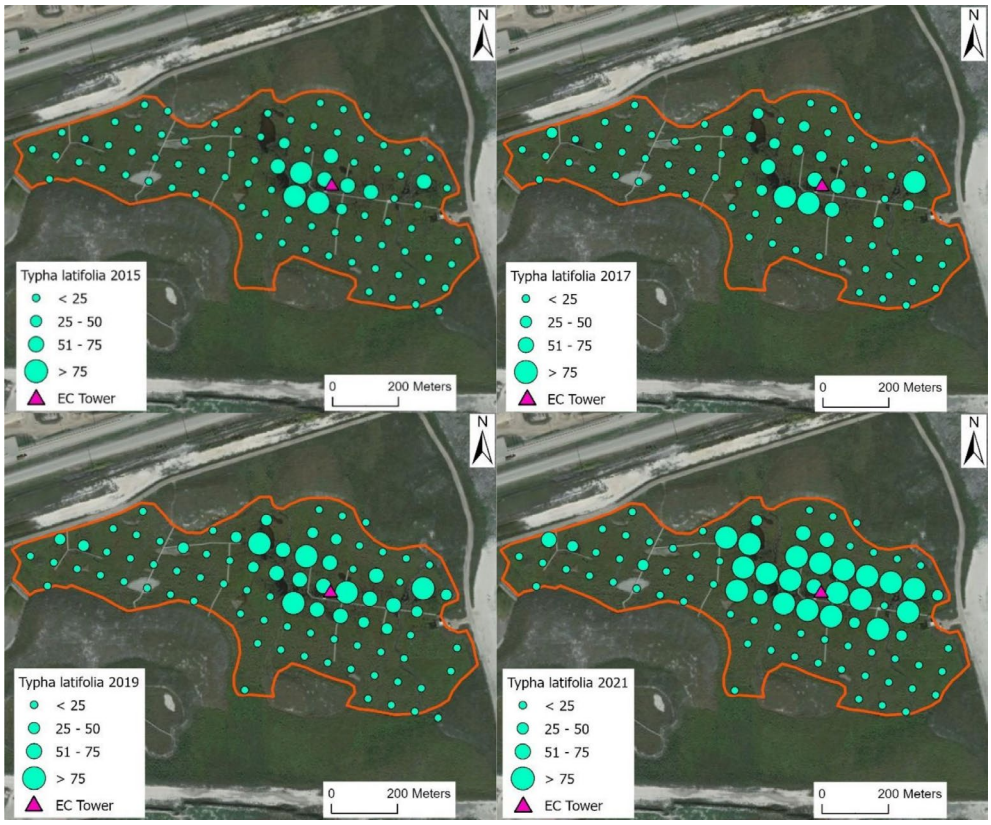


FIGURE 3 | Changes in *Typha latifolia* abundance (% of cover) in Sandhill Fen between 2015 and 2021.

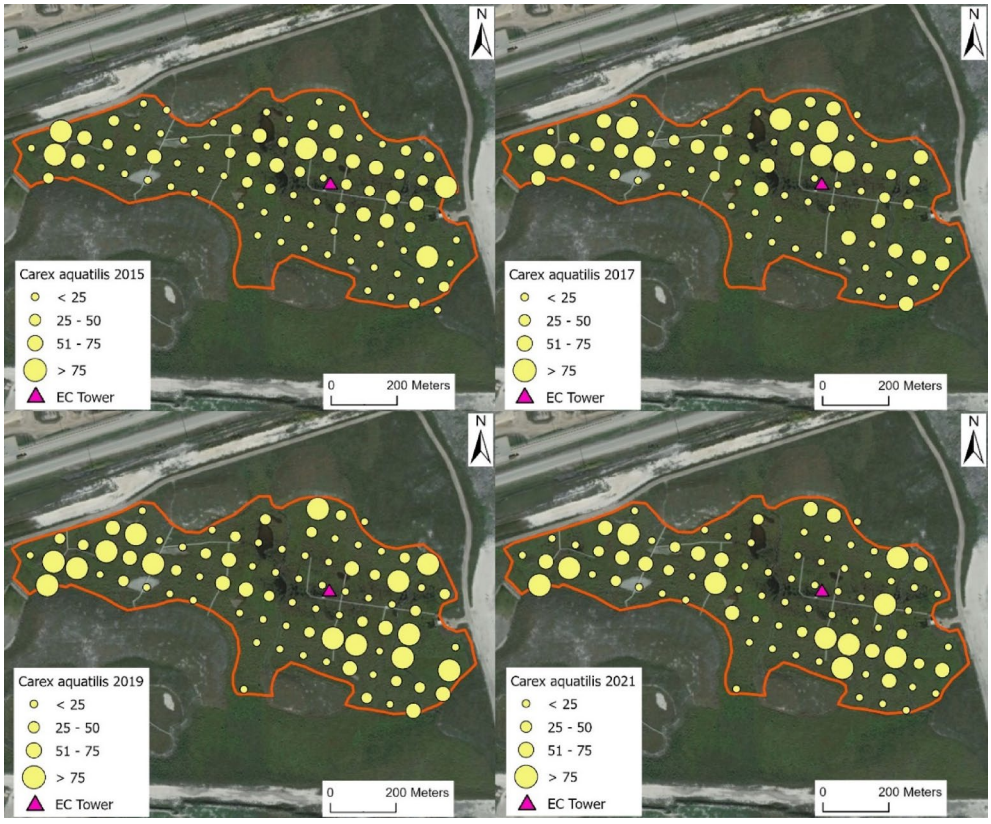


FIGURE 4 | Changes in *Carex aquatilis* abundance (% of cover) in Sandhill Fen between 2015 and 2021.

TABLE 1 | Study periods (April 1–October 31) for each year categorised based on temperature and precipitation conditions.

Climate conditions	2015	2017	2019	2021	2023
Warm	X	X			X
Cool			X		
Dry	X	X		X	
Wet			X		

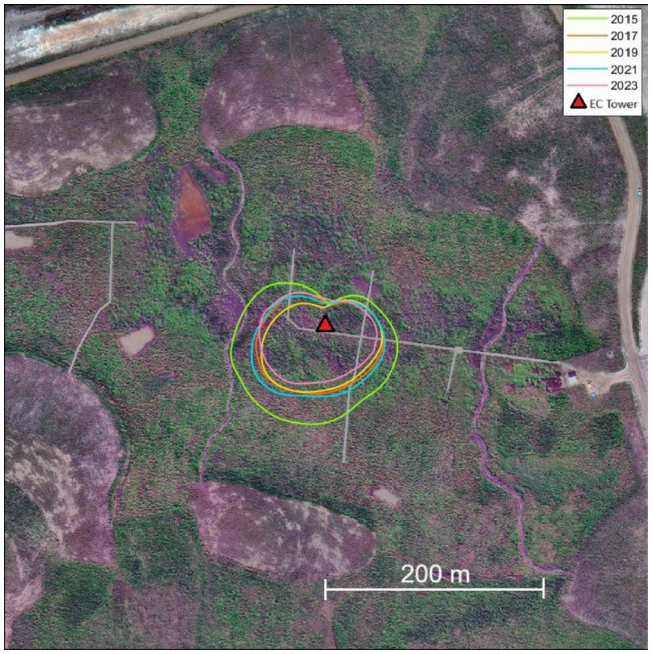


FIGURE 5 | 80% flux footprint for the EC tower between 2015 and 2021.

Among the five observed years, 2015 and 2017 were classified as warm and dry, while 2019 exhibited notably cool, wet conditions (Table 1). In 2021, dry conditions prevailed, though temperatures remained within the normal range. By contrast, 2023 was characterised by warm temperatures and normal precipitation conditions.

To compare environmental conditions across the study years, only midday values (11:00–15:00) were used for surface-atmosphere interaction parameters (i.e., g_a, g_s, and Ω). For energy fluxes, vapour pressure deficit, ET, and water table depth, daily data were used. The significance of intraseasonal and inter-annual changes in environmental variables was evaluated using the Kruskal–Wallis (KW) nonparametric statistical test (Kruskal and Wallis 1952), which was selected due to the violation of normality and homogeneity of variance assumptions in most of the data. For pairwise comparisons between individual months, we applied the Wilcoxon rank sum test, which evaluates differences based on magnitude-based ranks (Haynes 2013). These analyses were conducted in MATLAB R2024a using *kruskalwallis* and *ranksum* functions, respectively (MathWorks Inc.).

To assess changes in flux distances over time, we applied the footprint analysis method by Kljun et al. (2015). The measured fluxes were constrained within 80% of the study site boundaries (Figure 5). A progressive reduction in the flux footprint was observed, attributed to active vegetation growth, increased surface roughness, and a subsequent decrease in fetch. In 2015, the plots in the 80% footprint had a mean *Typha* coverage of 29%; but that increased in 2017 (39%), 2019 (50%), and again in 2021 (87%).

To evaluate the influence of environmental variables on the variability of ET in the Sandhill Fen, we employed the relative weight analysis (RWA) technique. RWA is a statistical method designed to quantify the relative contributions of predictor variables in a multiple regression model to the total coefficient of determination (R^2). This approach is particularly advantageous for addressing issues of multicollinearity among predictors (Tonidandel and LeBreton 2010).

In essence, RWA transforms the original predictors into a new set of orthogonal (uncorrelated) variables through principal component analysis. The dependent variable is then regressed on these orthogonal predictors. Subsequently, the resulting regression weights are transformed back to the scale of the original correlated predictors to estimate their contributions. The final step involves quantifying each predictor's contribution to the total R^2 by integrating transformed regression weights with their correlations to the dependent variable (Johnson 2000). For clarity, we expressed individual contributions as relative importance percentages in our analysis.

To ensure consistency between ET and its components (E and T), relative weight analysis was performed exclusively for the growing season (June 1–August 31), consistent with the period used for E and T partitioning. For this analysis, we selected seven environmental variables: air temperature, net radiation, vapour pressure deficit, the combined effect of VPD and wind speed (VPD × U), aerodynamic conductance, surface conductance, and water table depth. The analysis was conducted using measured (non-gap-filled) flux data.

Of note, while RWA is robust to multicollinearity, it does not explicitly address the key assumptions underlying linear regression, such as linearity, independence of errors, constant variance of errors, normality of residuals, and the absence of omitted variable bias. To address these assumptions and support the RWA results, we conducted an ordinary least squares (OLS) regression. However, it offered no additional insights or limitations beyond those identified by RWA and is included in the SI (Table S4).

3 | Results

3.1 | Microclimate

3.1.1 | Atmospheric Conditions

Across the five study periods, mean air temperature (T_a) was 12.4°C ± 1.0°C (±1 SD) (Table 2), approximately 1.5°C higher than the 1991–2020 climate normal for the same months at

TABLE 2 | Seasonal averages of environmental and energy flux variables, and total precipitation for the study period (April 1–October 31).

Variable	Units	2015	2017	2019	2021	2023	5-year average
T_{air}	°C	12.5	12.5	11.0	12.3	13.7	12.4
P_{tot}	mm	205	265	361	235	355	284
VPD	kPa	0.69	0.68	0.55	0.69	0.69	0.66
R_{Sdn}	MJ m^{-2} d^{-1}	16.8	15.9	14.9	15.5	15.1	15.6
R_n	MJ m^{-2} d^{-1}	9.15	8.80	8.22	9.20	8.18	8.71
LE	MJ m^{-2} d^{-1}	3.81	2.82	2.34	2.47	2.87	2.86
H	MJ m^{-2} d^{-1}	0.79	1.10	1.73	1.27	1.22	1.22
WT	masl	313.10	313.19	313.19	313.21	313.12	313.16

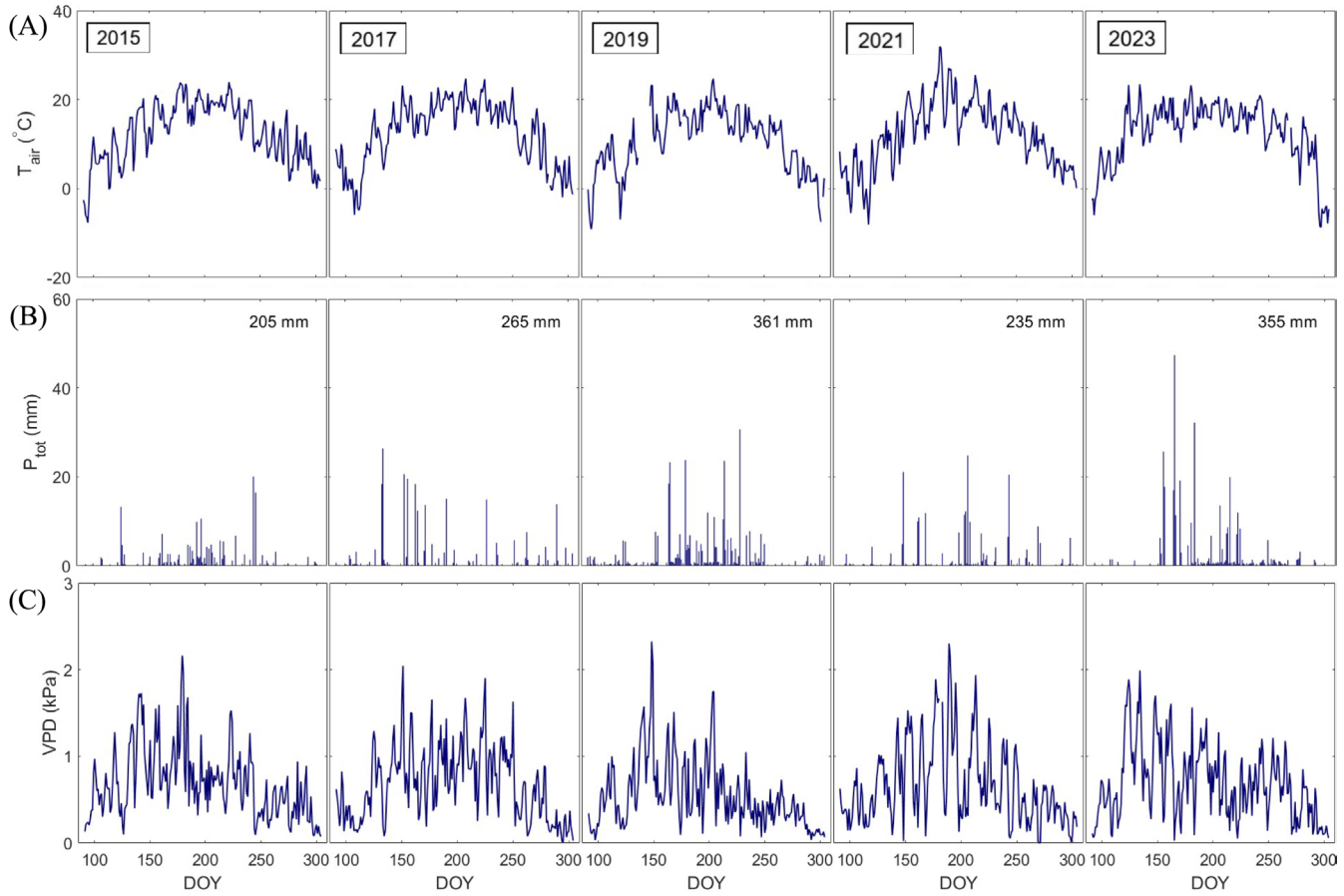


FIGURE 6 | Daily (April 1–October 31) air temperature (A) and precipitation (B) for the Mildred Lake Weather Station, and vapour pressure deficit (C) for the SFW.

Fort McMurray Airport (10.4°C). The warmest year was 2023 (13.7°C), while the coolest was 2019 (11.0°C; Figure 6A). Average growing season precipitation (P_{tot}) was 284 ± 71 mm, about 15% lower than the 30-year climate normal (330 mm). Wetter years (2019 and 2023) exceeded the climate normal, with 2019 receiving 361 mm, whereas drier years (2015, 2017, and 2021) recorded less than 270 mm, with 2015 being the driest (205 mm). Vapour pressure deficit (VPD) was relatively stable across the years, though elevated VPD occurred during summer in dry years and in late spring (April–May) during wetter years (Figure 6C).

3.1.2 | Water Table Dynamics

During the warm-dry years (2015 and 2017), the water table (WT) followed similar seasonal patterns—higher in spring, then gradually declining over the summer (Figure 7). In 2017,

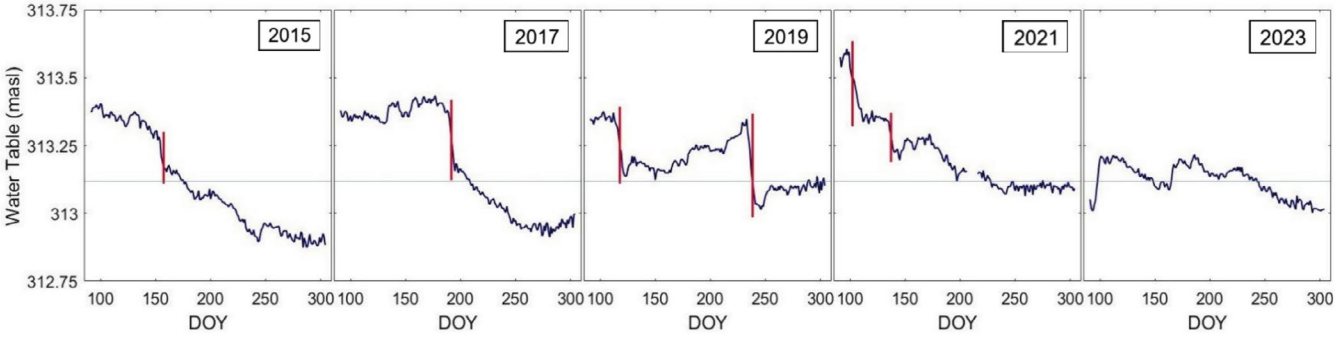


FIGURE 7 | Average daily (April 1–October 31) water table at Sandhill Fen. Vertical red lines indicate pumping events. The horizontal blue line represents the water level at the tower (313.12 masl).

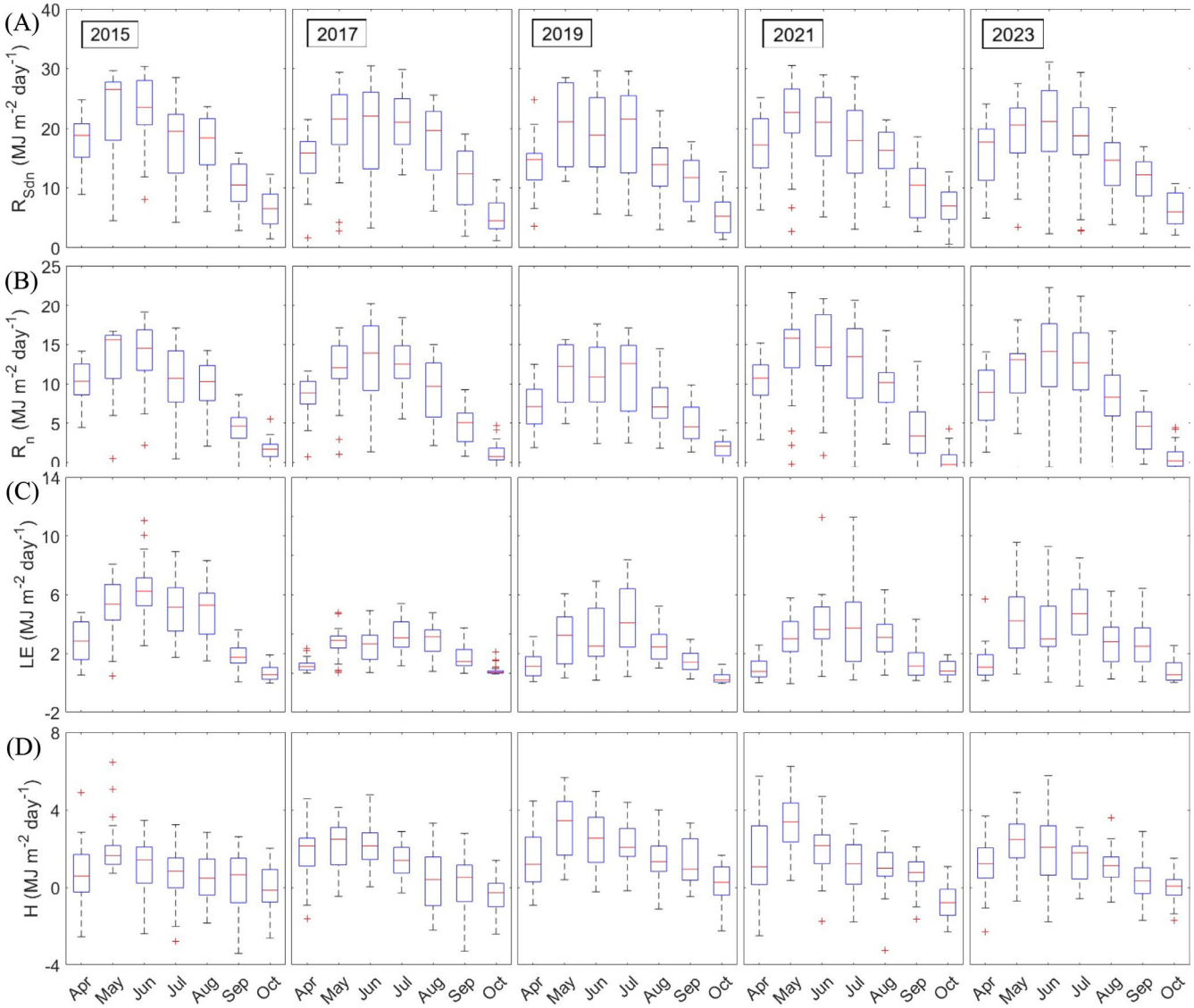


FIGURE 8 | Monthly box plots of daily (April 1–October 31) downwelling shortwave radiation (A), net radiation (B), latent (C), and sensible (D) heat fluxes.

the average WT was 0.09 m higher than in 2015 (Table 2). Sharp WT drops around DOY 160 (2015) and DOY 190 (2017) were linked to fen pumping activities (Biagi et al. 2021). Dry 2021 also showed declining WT, though levels stabilised earlier and remained generally higher. In contrast, cool-wet 2019 displayed a distinct pattern, with an early spring drop of −0.20 m (due to pumping), followed by a summer rise (DOY 152–243) driven by substantial rainfall (Figure 6B) and reduced evaporative

demand (Figure 8C), before another pumping event around DOY 234. Warm 2023 showed a similar pattern but with less seasonal WT variability.

3.2 | Surface Energy Fluxes

Warmer and drier years (2015, 2017, and 2021) had greater downwelling shortwave radiation (R_{Sdn}), reflecting clearer skies and increased energy input. Across all years, R_{Sdn} typically peaked in May and June. A Kruskal–Wallis test indicated significant variations in R_{Sdn} during April and August (KW, $p = 0.006$; Figure 8A). Net radiation (R_n) also had limited inter-annual variability, with the greatest intraseasonal differences occurring in October (KW, $p < 0.001$). The highest seasonal R_n values were recorded during the warm and dry periods of 2015 and 2021, while 2023 had the lowest seasonal mean (Table 2).

Turbulent heat fluxes (LE and H) exhibited notable variability throughout the study period, particularly at the intraseasonal scale. Across the 5 years, latent heat flux (LE) exhibited the greatest inter-annual variability during June and August (KW, $p < 0.001$), with peak monthly values generally occurring in July (Figure 8C). The post hoc analysis identified 2015 as significantly different from other years, consistent with the highest seasonal mean LE of 3.81 MJ m^{-2} d^{-1}, which corresponded to increased R_n and elevated VPD (Table 2). In contrast, sensible heat flux (H) exhibited its greatest variability in July (KW, $p < 0.001$), with marked differences between 2015 and 2019 (Figure 8D). After 2019, LE increased, reaching a higher seasonal value in 2023 due to warmer temperatures and elevated VPD. Meanwhile, H experienced a gradual decline, reaching 1.22 MJ m^{-2} d^{-1} in 2023 (Table 2).

Monthly LE and H fractions of R_n (LE/R_n and H/R_n) across the study periods showed that LE was the dominant contributor to the fen's energy budget during the growing season, reaching 0.50–0.75, and was lower (< 0.40) during the shoulder seasons (Table S2). In contrast, H contributions were generally lower in summer (< 0.35) but higher in spring and fall (0.20–0.50; Table S3). Notably, spring 2015 was an exception, with significant LE contributions even in April–May, while H played a lesser role in the energy balance during that period.

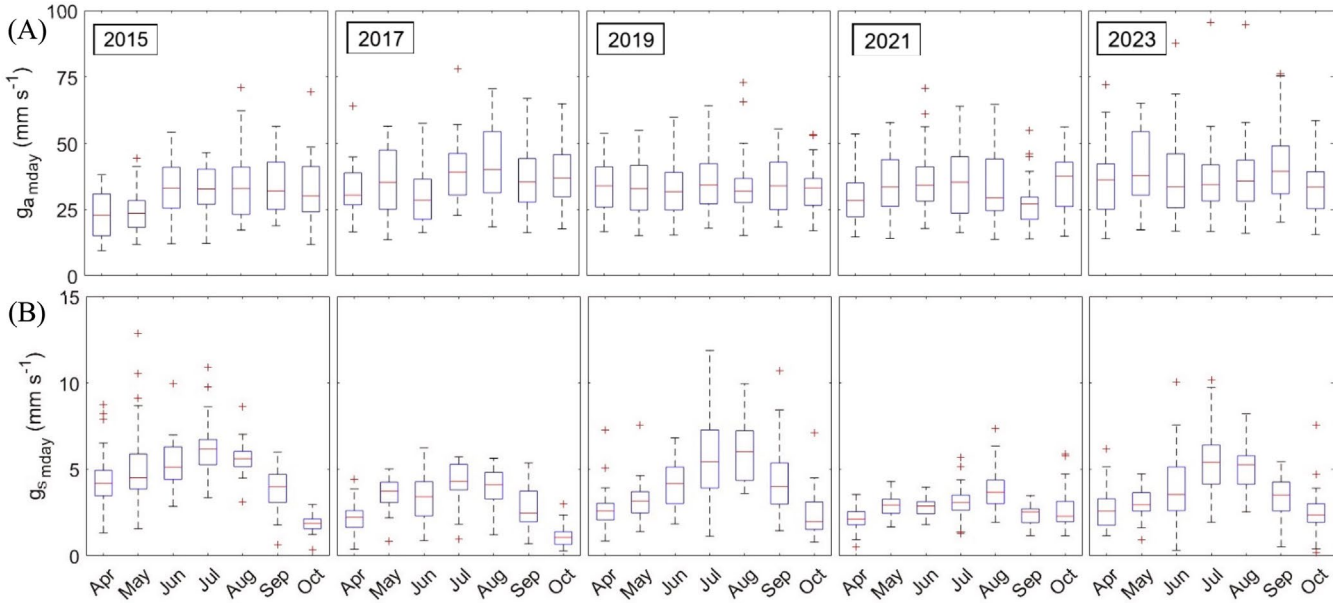


FIGURE 9 | Monthly box plots of daily midday (April 1–October 31) aerodynamic (A) and surface (B) conductance.

TABLE 3 | Seasonal averages (and totals) of ET, surface-atmosphere interaction terms, and vegetation cover during the study period (April 1–October 31).

Variable	Units	2015	2017	2019	2021	2023
ET_a	mm d^{-1} (mm)	1.55 (331)	1.15 (246)	0.95 (204)	1.01 (216)	1.17 (250)
ET_o	mm d^{-1} (mm)	3.12 (668)	2.92 (625)	2.56 (523)	2.98 (637)	2.73 (584)
$g_{a\,mday}$	mm s^{-1}	30.3	36.5	33.9	33.5	37.6
$g_{s\,mday}$	mm s^{-1}	4.64	3.04	4.09	2.86	3.72
Ω	—	0.32	0.21	0.24	0.20	0.23
Typha cover	%	19	28	36	63	—
Carex cover	%	32	27	19	13	—

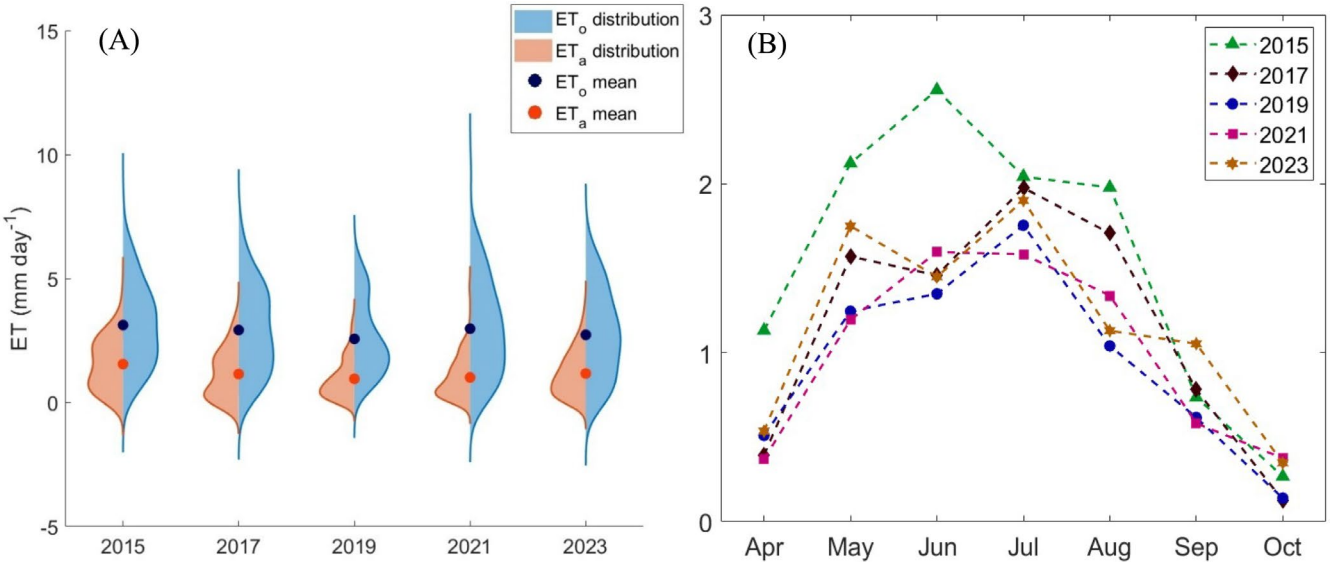


FIGURE 10 | Violin plots of daily (April 1–October 31) reference (ET$_o$) and actual (ET$_a$) evapotranspiration (A); average monthly ET$_a$ at SFW between 2015 and 2023 (B).

TABLE 4 | Seasonal average ET$_a$/ET$_o$ ratios for the study period (April 1–October 31).

Variable	2015	2017	2019	2021	2023
ET$_a$/ET$_o$	0.46	0.32	0.35	0.34	0.43

3.3 | Dynamics of Surface-Atmosphere Interactions

Aerodynamic conductance (g_a) exhibited distinct intraseasonal variability during fen ecosystem establishment, with the greatest fluctuations occurring during the shoulder season months, particularly May and September (KW, $p < 0.001$; Figure 9A). Post hoc analysis indicated that in spring (April–May), 2015 was the most distinct from the other years, while September 2021 also showed significant differences. These variations during the shoulder seasons are likely linked to dormant vegetation in spring and the onset of senescence in fall. The highest mean g_a was recorded in 2023 (37.6 mm s^{-1}), reflecting the rapid growth of *Typha latifolia*.

Surface conductance (g_s) displayed greater intraseasonal variability than g_a, with statistically significant differences across all months. Variability was highest during the summer months (June–August; KW, $p < 0.001$), with peak monthly means in July (Table S1), coinciding with maximum vegetation growth (Figure 9B). Declines in seasonal g_s were observed during drier years, although this was not the case in 2015, possibly due to elevated LE and the dominance of *Carex* near the EC tower (Table 3). In contrast, elevated g_s was associated with wetter conditions and ample water availability, despite decreased LE and VPD (e.g., in 2019).

Throughout the study, the fen exhibited an intermediate degree of coupling with the atmosphere, with mean seasonal decoupling coefficient (Ω) values ranging from 0.20 (2021) to 0.32 (2015). The highest Ω values were observed in July ($\Omega_{max} = 0.41$ in July 2015; Table S1), coinciding with elevated g_s in 2015, 2017, and 2023, while lower values occurred during the shoulder seasons (Figure S2) when g_s declined. The peak Ω suggests that ET was predominantly controlled by VPD and surface characteristics (i.e., g_a and g_s). This is further supported by the stronger influence of VPD on summer ET at SFW compared to R_n (Figure 12).

3.4 | ET Dynamics

Both reference and actual evapotranspiration (ET$_o$ and ET$_a$) exhibited notable inter-annual variability. ET$_a$ showed greater fluctuations (KW, $p < 0.001$; Figure 10A), primarily driven by significant differences between mean ET$_a$ values in 2015 and the subsequent 4 years, as indicated by post hoc analysis. The **5-year** average total ET$_a$ was 249 ± 49.9 mm, with the highest rate of 331 mm observed during the driest 2015, and the lowest at 204 mm in the cool and wet 2019. In contrast, changes in ET$_o$ were less pronounced (KW, $p = 0.02$; Figure 10A), with the largest differences observed between 2015 and 2019.

ET$_a$ declined by approximately 40% between 2015 and 2019, while ET$_o$ decreased by around 20% over the same period. After 2019, ET$_o$ increased in 2021, though not significantly (Wilcoxon, $p = 0.06$), and showed no notable change afterward ($p = 0.28$). In contrast, ET$_a$ increased significantly by about 20% between 2019 and 2023 (Wilcoxon, $p = 0.01$).

Intra-seasonal ET variations varied across the study years. The greatest variability in both ET$_a$ and ET$_o$ occurred in dry years (2015 and 2021). The median ET$_a$ in 2015 was 1.45 mm d^{-1}, with an interquartile range (IQR) of 0.64–2.35 mm d^{-1}, while the median ET$_o$ in 2021 was 2.76 mm d^{-1}, with an IQR of 1.33–4.28 mm d^{-1}. Conversely, 2019 exhibited the lowest variability, with a median ET$_a$ of 0.75 mm d^{-1} (IQR: 0.36–1.37 mm d^{-1}) and a median ET$_o$ of 2.22 mm d^{-1} (IQR: 1.36–3.59 mm d^{-1}),

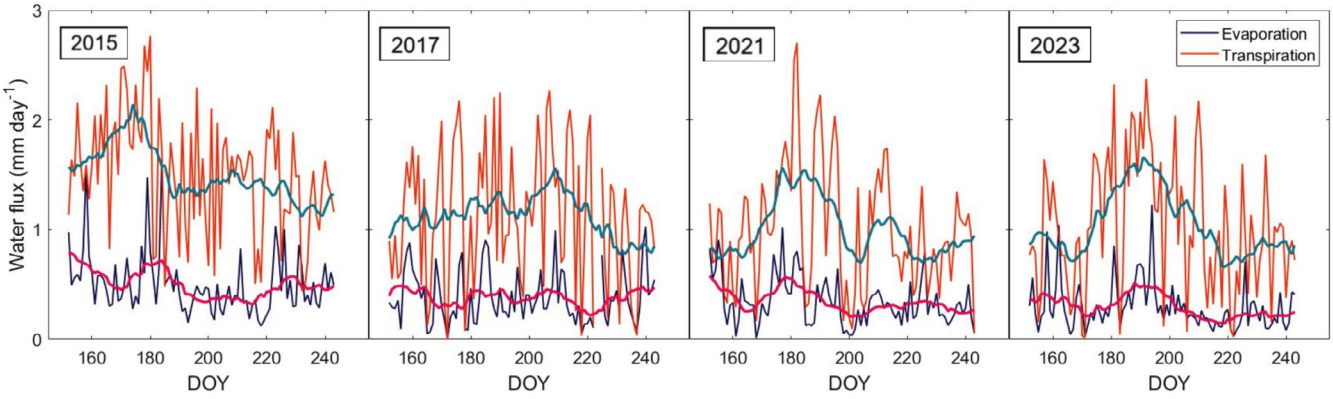


FIGURE 11 | Average daily growing season (June 1–August 31) evaporation and transpiration at Sandhill Fen. Red and green lines represent 14-day running means for *E* and *T*, respectively. High-frequency data for the summer of 2019 were missing due to limited site access and were therefore excluded.

TABLE 5 | Seasonal averages (and totals) of *E* and *T* for the growing season (GS) and the month of July.

Variable	Units	2015	2017	2021	2023
E_{GS}	mm d^{-1} (mm)	0.50 (46.3)	0.38 (34.6)	0.35 (31.9)	0.30 (27.7)
E_{July}		0.44 (13.8)	0.43 (13.4)	0.31 (9.75)	0.66 (11.2)
T_{GS}		1.50 (138)	1.12 (101)	1.00 (92.2)	1.04 (95.4)
T_{July}		1.40 (43.5)	1.30 (40.3)	1.12 (34.7)	1.35 (42.0)

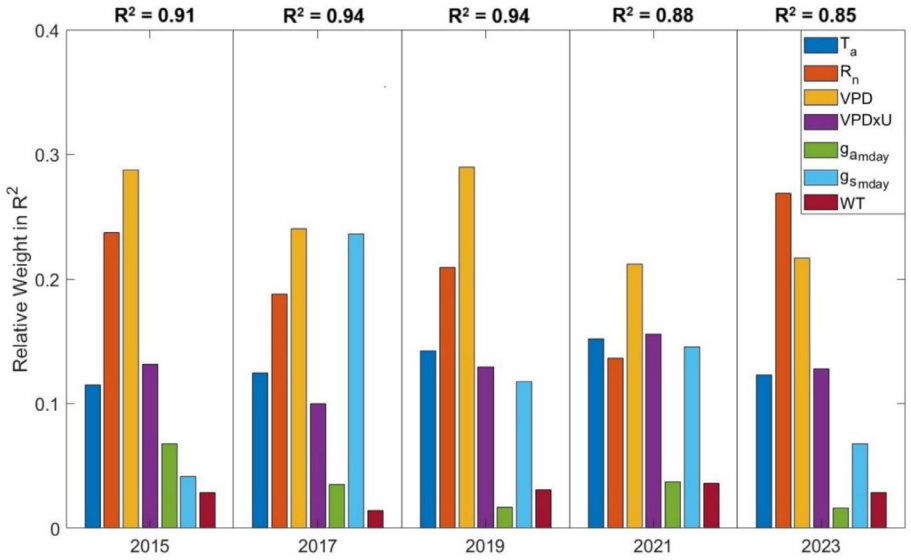


FIGURE 12 | Relative weight distribution of environmental variables contributing to ET during the growing season (June 1–August 31).

representing the lowest ET across study periods. The mean seasonal ET_a/ET_o ratio across the five study periods was 0.38, with 2015 exhibiting the highest value ($ET_a/ET_o = 0.46$; Table 4).

3.5 | Growing Season *E* and *T*

Growing season transpiration (*T*) varied significantly across years (KW, $p < 0.001$; Figure 11), with 2015 showing the largest difference. The 4-year mean *T* was 1.17 ± 0.23 mm d^{-1}, peaking in 2015 (1.50 mm d^{-1}). Following 2015, *T* declined, reaching a minimum in 2021 (1.00 mm d^{-1}; Table 5), before increasing by 2023, though the change was not significant (Wilcoxon, $p = 0.28$).

Seasonal T peaked in early to mid-summer (DOY 170–200), with the highest rate recorded in 2015 (2.77 mm d^{-1} on DOY 181). An exception occurred in 2017, when elevated T persisted between DOY 200 and 220, likely due to increased g_s during July and August

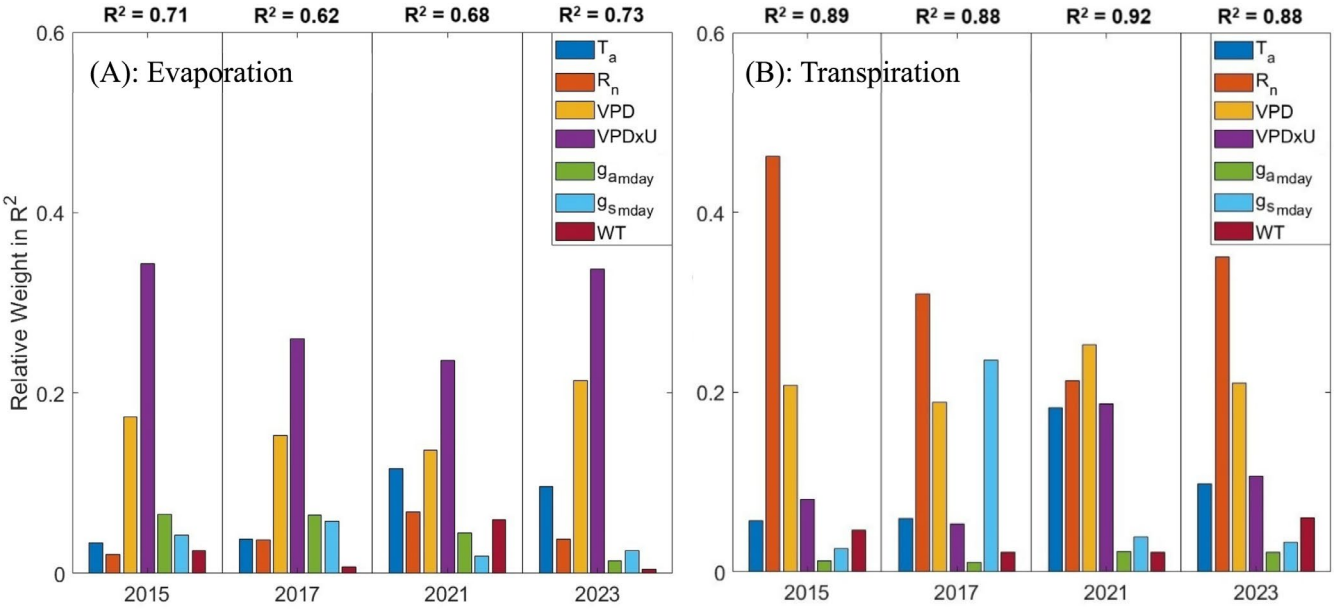


FIGURE 13 | Relative weight distribution of environmental variables contributing to (B): transpiration (A): evaporation (A) and transpiration (B) during the growing season (June 1–August 31).

(Figure 9B). In contrast, a sharp drop in T around DOY 200 in 2021 coincided with reduced VPD (Figure 6C), reflecting the stronger influence of VPD on T during that period (Figure 13B).

Evaporation (E) also varied significantly across years (KW, $p < 0.001$), with the highest rates in 2015. The mean E was $0.38 \pm 0.09\,\mathrm{mm\,d^{-1}}$, declining from $0.50\,\mathrm{mm\,d^{-1}}$ during the dry summer of 2015 to $0.30\,\mathrm{mm\,d^{-1}}$ in the wet season of 2023 (Table 5). Elevated E typically occurred between DOY 170 and 220; although the timing varied across the years. The highest rate was recorded in June 2015 ($1.64\,\mathrm{mm\,d^{-1}}$; DOY 185). Despite the notably wet summer of 2023, E remained lower than in 2015 and 2017.

3.6 | Relative Weight Analysis

Over the growing season, relative weight analysis indicated that climate variables explained 85%–94% of the variability in ET, depending on the year (Figure 12). Specifically, VPD made the highest relative contribution to the explained variance in ET in 4 out of 5 years, accounting for approximately 28% of its variability. Net radiation contributed more substantially to ET variability during the cool and wet 2023, accounting for 32% of its explained variance. Additionally, R_n influenced ET during the dry conditions of 2015 and the cool, wet conditions of 2019, accounting for ~25% of ET variability. T_a and VPD × U exhibited similar relative importance, with an average contribution of 14%–15% across the 5 years.

Surface conductance (g_s) made a notable contribution to ET variability in 2017, explaining approximately 25% of the variance; while in 2021, it ranked fourth, behind VPD, VPD × U, and T_a, with a contribution of 17%. Neither g_a nor WT contributed meaningfully to the explained variance in ET in any year.

During the summer months, fen evaporation, as derived from the flux partitioning analysis, was most strongly associated with the combined effect of VPD and U across all 4 years, explaining approximately 43% of the variance in E (Figure 13A). VPD alone was the second most influential variable in all growing seasons, with a mean relative contribution of 25%. Notably, in 2015 and 2017, g_a ranked third in relative importance, accounting for ~10% of the explained variance. In contrast, T_a replaced g_a in 2021 and 2023, contributing slightly more (~15%). This shift may reflect the warmer conditions during these years. Other variables had a minimal influence on E, with relative importance scores ranging from 2% to 10%.

In contrast, growing season transpiration as derived from the flux partitioning analysis was predominantly influenced by R_n, particularly in 2015, 2017, and 2023 (Figure 13B). During the warm and dry 2015, R_n accounted for over 50% of T variability. In 2021, however, VPD had the highest relative contribution to the explained variance in T, accounting for approximately 30%; while R_n ranked second. In 2017 only, g_s was a major contributor, explaining 27% of the variability in T. T_a and VPD × U also played notable roles in 2015, 2021, and 2023, with increased importance during the warm conditions of 2021. Neither g_a nor WT was a significant influence on T variability in any of the study years.

4 | Discussion

4.1 | Primary Environmental Factors Regulating Growing Season ET

4.1.1 | Seasonal and Interannual Dynamics of ET at Sandhill Fen

ET at Sandhill Fen has shown considerable variability both within and among years. The April–September mean ET (231 ± 45 mm) aligns with values reported for a natural peatland in northern Alberta (237 mm; Brown et al. 2010) and a boreal fen in Manitoba, Canada (250 mm; Lafleur et al. 1997). Seasonal ET during dry and wet periods at SFW (237 and 204 mm,

respectively) was lower than that of a peatland complex in eastern Finland (347 mm in a dry year, 246 mm in a wet year; Wu et al. 2010), likely due to a higher proportion of open water in the latter.

In all years except 2015, rainfall exceeded ET. Peak ET typically occurred in early to mid-summer (June–July), with much lower rates in the shoulder months (April and October; Figure 10B), driven by lower radiation, air temperatures, and VPD (Figures 6 and 8A). Notably, July total ET at SFW in 2015 and 2017 was lower (Table S1) than in undisturbed treed fens in the AOSR (~80–100 mm), but comparable to a nearby open fen (~65 mm) reported by Volik, Petrone, et al. (2021) for the same years. Given the shared regional climate, Sandhill Fen's resemblance to an open fen reflects the greater open-water coverage during the early years of monitoring and the transitional stage of *Typha* establishment, which could limit transpiration and overall water loss.

ET also varied among years, particularly in response to prevailing temperature and precipitation conditions (Figure 10A). In dry years, ET was approximately 15% higher than in wet years, consistent with the trends observed by Wu et al. (2010). However, our results contrast with findings from a sedge-dominated natural fen in Manitoba, where ET increased during wetter years with higher precipitation and water availability (Eaton and Rouse 2001). This discrepancy may reflect differences in environmental context (e.g., coastal location) and methodological approaches, as Eaton and Rouse (2001) used the Bowen Ratio-Energy Balance (BREB) method, which assumes uniform flux distribution and static gradients (Tomlinson 1996), assumptions often violated in heterogeneous wetland environments with complex microtopography.

There were notable differences observed between reference and actual evapotranspiration. Modelled ET_o was consistently higher than ET_a during drier periods (Figure 10A and Table 3), highlighting considerable variation in water loss efficiency across years (Table 4). These discrepancies could result from the wetland-specific microclimatic conditions, such as increased near-surface humidity, which reduces VPD and ET_a, and tall vegetation that shades open water, thereby reducing vapour exchange (Kelvin et al. 2017), both of which were observed at Sandhill Fen.

Flux variance partitioning results revealed that transpiration consistently exceeded evaporation during the growing season, as indicated by high T/ET ratios (0.68–0.72; Figure S3), which are greater than those reported for wetlands in northern Wisconsin and Central Europe (0.45–0.49; Lu et al. 2023; Shveytser et al. 2024). While site-specific conditions may partly explain these differences, the methodological approach likely plays a greater role. The abovementioned studies relied on EC combined with machine learning (XGBoost) and flux-variance similarity (FVS). XGBoost improves large-scale partitioning by avoiding assumptions about water–carbon flux coupling and incorporating diverse inputs (e.g., air temperature, VPD, vegetation indices; Lu et al. 2023). However, FVS can be less reliable in heterogeneous environments due to the potential decoupling of scalar fluxes and variances, making it less accurate than the CEC method, which directly captures flux contributions from turbulent updrafts and downdrafts (Zahn et al. 2022).

4.1.2 | Microclimate Controls on Growing Season ET

Our results indicate that growing season ET was primarily influenced by atmospheric conditions, particularly vapour pressure deficit and net radiation (Figure 12 and Table S4). VPD was more influential, especially under warmer and drier conditions, consistent with findings by Helbig et al. (2020), who showed that VPD played a key role in regulating ET variability across boreal peatlands during dry periods through its impact on surface conductance. At SFW, VPD remained relatively elevated throughout the study; however, ET did not respond as strongly, likely due to the lack of mosses and their associated negative feedbacks to drying. Of note, under wetter conditions, ET was influenced by both VPD (in 2019) and R_n (in 2023). The high sensitivity to VPD in 2019 reflects overall low VPD under wet conditions, while the increased importance of R_n in 2023 corresponds to greater cloud cover that limited energy input. A similar interplay between VPD, R_n, and ET was reported by Volik, Kessel, et al. (2021), who found that during warmer years, ET from natural fens in the AOSR was strongly correlated with both variables, further highlighting their importance in influencing ET during varying temperature and precipitation conditions.

When assessing the influence of the water table on ET, RWA results indicate that, despite notable temporal variability (Figure 7), it was not an influence on ET variability at SFW. This is further supported by the lack of significant statistical relationships between the two variables in most study years (Table S4). A likely explanation is the consistently high water table near the tower, resulting in open water during low WT periods. These findings align with other studies in the AOSR, which also reported weak correlations between WT and ET across multiple wetland sites under persistently saturated conditions (Scarlett et al. 2017; Volik, Kessel, et al. 2021).

To better understand the mechanisms underlying total ET, we examined the environmental variables influencing its two main components—evaporation (E) and transpiration (T)—individually. Notably, each component responded to a distinct set of atmospheric variables. E variability responded to air temperature and the VPD × U interaction term (Figure 13A). T_a contributed notably in 2021 and 2023, underscoring the role of warm conditions in promoting open-water evaporation. In turn, the VPD × U explained the largest portion of E variability across all years. To assess potential collinearity, RWA was conducted without the VPD × U interaction term. This reduced the coefficient of determination for the E model only, suggesting that stomatal regulation buffers wind effects on T but not on E (analysis not shown). The strong influence of VPD and U on E is well documented in wetlands with extensive open-water areas (Price 1994; Liljedahl et al. 2011), where wind enhances E by disrupting the saturated boundary layer. This is further supported by findings from open-water systems (e.g., lakes), where the VPD × U explained ~75% of daily LE variability and U was a key factor in evaporation modelling accuracy (Clark et al. 2021; Clark and Carey 2024).

In contrast to evaporation, transpiration at SFW was primarily influenced by R_n and VPD. R_n explained a substantial portion of T variability, with particularly strong contributions during dry and wet years (Figure 13B). These findings align with previous studies in boreal peatlands, where T comprises the larger share of total ET and R_n explains much of its variability (Sonnentag et al. 2010; Moore et al. 2013). Although fewer studies have focused specifically on the relationship between VPD and T in the peatlands, evidence from shrublands and forest ecosystems supports its importance (Nicholls et al. 2023). In their study, VPD had a stronger influence during the growing season in shrublands and the shoulder seasons in spruce forests, when vegetation was less developed. This seasonal modulation of VPD influence aligns with our observations at SFW, where both R_n and VPD emerged as key drivers of T, with their limiting effects pronounced under wet and cloudy conditions.

4.2 | Inter-Annual ET Variability in Response to Shifts in Dominant Plant Communities and Regional Climate Conditions

While climate variables largely influence ET at SFW, changes in surface properties and vegetation also play a crucial role. Our data show a decline in growing season (June–August) total ET between 2015 and 2023. This reduction may be attributed to the expansion of *Typha latifolia* near the EC tower (Table 3). The presence of *Typha* in wetlands has been shown to suppress ET by sheltering open water and reducing wind-driven evaporation (Nichols and Brown 1980). Although total ET responded weakly to aerodynamic conductance (Figure 12 and Table S4), g_a influenced E variability (Figure 13A), particularly in 2015 and 2017, when sparse vegetation and open water likely enhanced g_a and promoted E. In contrast, by 2021 and 2023, g_a contribution to E variability declined, suggesting that reduced open-water areas and increased *Typha* shading shifted control towards atmospheric forcing.

In addition to changes in surface conditions, vegetation characteristics can significantly regulate ET in the peatlands. This study assessed surface conductance to evaluate the impact of vegetation shifts on ET. The influence of g_s on ET was stronger in warm and dry years (Figures 12 and 13B), when reductions in g_s, likely due to water retention by *Typha*, led to suppressed ET and T fluxes (Figure 10B). Similar declines in ET associated with increased stomatal resistance were observed in other peatland ecosystems, including a constructed fen in the AOSR (Scarlett et al. 2017), a natural wetland with diverse vegetation in north-central Alberta (Brown et al. 2010), and *Typha*-dominated peatlands (Goulden et al. 2007). These findings are consistent with the patterns observed in our study but may not reflect typical ET responses across all wetland types.

While g_s explained a large portion of ET variability during drier periods, its overall influence was limited in most other years, likely due to consistently high water tables (Figure 7). These persistently wet conditions favour *Typha latifolia*, which is likely to continue expanding under the current management. Highly adaptable, *Typha* tolerates fluctuating water levels, prolonged flooding, and drawdowns (Bansal et al. 2019)—conditions typical of Sandhill Fen. Though often used in wetland restoration for its nutrient-regulating capacity, *Typha* dominance can suppress plant diversity by increasing litter accumulation, nitrogen levels, and shading (Mollard et al. 2013; Graham et al. 2022). While further expansion of *Typha* may help limit water loss at SFW, it could also outcompete native fen species, such as grasses and sedges, thereby altering ecosystem structure. As a result, Sandhill Fen may continue evolving into a marsh-like wetland, potentially diverging from reclamation goals aimed at restoring a peat-accumulating, drought-resilient fen ecosystem.

4.3 | Hydrological Function of the Sandhill Fen

To assess the hydrological function of Sandhill Fen, we evaluated surface–atmosphere interactions and energy partitioning, alongside ET, in the context of other peatlands. In our study, May–September ET during the first year (2015) was lower than the 350 mm reported for SFW in its initial 2 years post-commissioning (2013–2014; Nicholls et al. 2016) and the 330–420 mm observed at Nikanotee Fen, another constructed wetland in the region (Scarlett et al. 2017; Popović et al. 2022, 2025). The higher ET rates reported in those studies were attributed to wet, dark peat surfaces and extensive open water areas. In later years (e.g., 2017 and 2019), ET at Nikanotee Fen declined as vegetation cover developed (Popović et al. 2022) but remained higher than the ET observed at SFW during the same period, possibly due to the greater abundance of *Typha* at Sandhill Fen.

Surface-atmosphere interactions at SFW differed from both constructed and natural peatlands. The decoupling coefficient was generally lower during drier years, coinciding with reduced g_s and indicating stronger surface control on ET (Table 3). A similar pattern was observed at Nikanotee Fen, where vegetation establishment also weakened atmospheric coupling, although seasonal Ω values were slightly higher (0.32–0.49; Popović et al. 2023), likely due to differences in plant community composition and surface wetness. At SFW, seasonal Ω fell within the range reported for undisturbed boreal peatlands (0.20–0.50; Kurbatova et al. 2002; Alekseychik et al. 2018), aligning more closely with natural fens than bogs, reflecting contrasts in dominant vegetation and their response to moisture stress.

Notable interannual shifts in energy partitioning were observed at SFW, with latent heat flux contributing more prominently in most years. Our estimates were slightly lower (Table S2) than those reported for Nikanotee Fen 5–7 years post-reclamation (Popović et al. 2023) and aligned more closely with values from undisturbed, moderately open, sedge-dominant fens in the AOSR (LE/R_n: 0.40–0.60; Volik, Petrone, et al. 2021). Reduced LE contributions in 2017 and 2021 were likely linked to drier conditions. A decline in LE/R_n ratio under such conditions, reflecting increased energy allocation to sensible heat flux, has been reported in natural peatlands in north-central Alberta (Petrone et al. 2007; Morison et al. 2020). At SFW, elevated seasonal H/R_n ratios were particularly notable in 2019 and 2021 (Table S3). In 2021, this increase likely resulted from warmer, moderately dry conditions and suppressed LE flux, whereas in 2019, the elevated H/R_n ratio likely reflected a combination of reduced LE, decreased radiation due to cloud cover, and lower aerodynamic conductance (Tables 2 and 3).

Considering the importance of wetland reestablishment in the AOSR and the observed variability in ET, vegetation composition, surface-atmosphere interactions, and energy partitioning, several management strategies may help sustain hydrological function at SFW and improve reclamation outcomes. Post-construction management should prioritise promoting vegetation communities that enhance transpiration and ecosystem–atmosphere coupling. In particular, limiting the dominance of *Typha latifolia* by encouraging *Carex aquatilis* establishment in wetter areas could reduce the risk of *Typha* encroachment, as targeted planting of *Carex* has been shown to perform well under wetter conditions (Vitt et al. 2011; Borkenhagen et al. 2024). Active *Typha* management, such as manual biomass removal in areas of extensive invasion, may further mitigate its spread (Graham et al. 2022). Maintaining stable, shallow water tables is also critical to support fen-native vegetation and hydrological function (Ketcheson et al. 2016). Long-term reclamation planning should account for interannual climate variability and include hydrometeorological monitoring across wet, average, and dry years to assess ecosystem resilience. Implementing adaptive management strategies, such as periodic reassessment of site conditions and timely interventions, can improve long-term fen function and resilience (Wardekker et al. 2016).

5 | Conclusions

This study examines multi-year ET and energy dynamics in a reclaimed boreal wetland, offering insights into hydrological changes following disturbance. Our findings indicate that growing season ET was up to 15% higher during warmer and drier years, with the lowest rates observed in the coolest and wettest year. Mean seasonal ET over the study period was 249 ± 49.9 mm, consistent with estimates from natural and constructed boreal peatlands. Intra-annual ET variability was primarily influenced by vapour pressure deficit and net radiation, while its long-term decline corresponded with an increase in *Typha latifolia* cover near the tower, from 19% to 63%. Partitioning results showed that transpiration accounted for approximately 70% of total ET, suggesting that the emergent structure of *Typha* reduced water loss by sheltering the surface and limiting both radiative input and turbulent exchange. Although ET declined over the study period, the energy balance at SFW remained largely dominated by latent heat flux, indicating that Sandhill Fen is progressing toward functional similarity with natural wetlands in terms of hydrological behaviour. Rainfall exceeded ET in 80% of the years, reflecting generally sufficient moisture availability and the absence of prolonged drought.

In light of the ongoing expansion of reclamation projects in the AOSR, accurately quantifying vertical water loss through ET is critical for informing the design and long-term sustainability of constructed wetlands. This study provides a detailed assessment of water and energy fluxes in a constructed fen, offering insights into surface-atmosphere interactions and the magnitude of water loss from the system. By partitioning ET, the analysis reveals key environmental drivers of water loss and highlights how shifts in vegetation structure, particularly the establishment of non-native peatland species, can influence fen microclimate. Although broader hydrological connectivity is not addressed, the findings emphasise the importance of ongoing flux and vegetation monitoring to refine reclamation strategies and improve future wetland planning.

Acknowledgements

Site access, archived data, and funding were provided by Syncrude Canada Ltd. We also thank Dr. Mike Treberg and Dr. Gordon Drewitt for site maintenance and data management. Additionally, we extend our gratitude to Melissa House for providing vegetation survey data.

Conflicts of Interest

The authors declare no conflicts of interest.

Data Availability Statement

The data that support the findings of this study are available from the corresponding author upon reasonable request.

References

Alberta Environment and Parks (AEP). 2018. Oil Sands Monitoring Program. Annual Report for 2017–2018. [Online]. https://open.alberta.ca/dataset/dbe8811a-962e-4ce1-b2c2-ff40b8daad7a/resource/35be7d6d-083e-4d28-bf89-b92a7f3ab759/download/osm-annual-report-2017-2018-signed-by-aep-eccc.pdf.

Alekseychik, P., I. Mammarella, A. Lindroth, et al. 2018. "Surface Energy Exchange in Pristine and Managed Boreal Peatlands." *Mires and Peat* 21, no. 14: 1–26. https://doi.org/10.19189/MaP.2018.OMB.333.

Allen, R., L. Pereira, D. Raes, and M. Smith. 1998. *FAO Irrigation and Drainage Paper No. 56*, 26–40. Food and Agriculture Organization of the United Nations. 56.

Amaro Medina, D., and S. K. Carey. 2024. "Long-Term Evaluation of Evapotranspiration From a Reclaimed Boreal Forest in the Athabasca Oil Sands Region of Northern Alberta, Canada." *Journal of Hydrology: Regional Studies* 56: 102073. https://doi.org/10.1016/j.ejrh.2024.102073.

Bansal, S., S. C. Lishawa, S. Newman, et al. 2019. "Typha (Cattail) Invasion in North American Wetlands: Biology, Regional Problems, Impacts, Ecosystem Services, and Management." *Wetlands* 39, no. 4: 645–684. https://doi.org/10.1007/s13157-019-01174-7.

Biagi, K. M., and S. K. Carey. 2020. "The Role of Snow Processes and Hillslopes on Runoff Generation in Present and Future Climates in a Recently Constructed Watershed in the Athabasca Oil Sands Region." *Hydrological Processes* 34, no. 17: 3635–3655. https://doi.org/10.1002/hyp.13836.

Biagi, K. M., M. G. Clark, and S. K. Carey. 2021. "Hydrological Functioning of a Constructed Peatland Watershed in the Athabasca Oil Sands Region: Potential Trajectories and Lessons Learned." *Ecological Engineering* 166: 106236. https://doi.org/10.1016/j.ecoleng.2021.106236.

Biagi, K. M., C. J. Oswald, E. M. Nicholls, and S. K. Carey. 2019. "Increases in Salinity Following a Shift in Hydrologic Regime in a Constructed Wetland Watershed in a Post-Mining Oil Sands Landscape." *Science of the Total Environment* 653: 1445–1457. https://doi.org/10.1016/j.scitotenv.2018.10.341.

Borkenhagen, A., D. J. Cooper, M. House, and D. H. Vitt. 2024. "Establishing Peat-Forming Plant Communities: A Comparison of Wetland Reclamation Methods in Alberta's Oil Sands Region." *Ecological Applications* 34, no. 2: e2929. https://doi.org/10.1002/eap.2929.

Bourgeois, B., S. Hugron, and M. Poulin. 2012. "Establishing a Moss Cover Inhibits the Germination of *Typha latifolia*, an Invasive Species, in Restored Peatlands." *Aquatic Botany* 100: 76–79. https://doi.org/10.1016/j.aquabot.2012.03.010.

Brown, S. M., R. M. Petrone, C. Mendoza, and K. J. Devito. 2010. "Surface Vegetation Controls on Evapotranspiration From a Sub-Humid Western Boreal Plain Wetland." *Hydrological Processes* 24, no. 8: 1072–1085. https://doi.org/10.1002/hyp.7569.

Carey, S. K. 2008. "Growing Season Energy and Water Exchange From an Oil Sands Overburden Reclamation Soil Cover, Fort McMurray, Alberta, Canada." *Hydrological Processes* 22, no. 15: 2847–2857. https://doi.org/10.1002/hyp.7026.

Cavanaugh, M. L., S. A. Kurc, and R. L. Scott. 2011. "Evapotranspiration Partitioning in Semiarid Shrubland Ecosystems: A Two-Site Evaluation of Soil Moisture Control on Transpiration." *Ecohydrology* 4, no. 5: 671–681. https://doi.org/10.1002/eco.157.

Clark, M. G., and S. K. Carey. 2024. "An Open-Source Refactoring of the Canadian Small Lakes Model for Estimates of Evaporation From Medium-Sized Reservoirs." *Geoscientific Model Development* 17, no. 12: 4911–4922. https://doi.org/10.5194/gmd-17-4911-2024.

Clark, M. G., G. B. Drewitt, and S. K. Carey. 2021. "Energy and Carbon Fluxes From an Oil Sands Pit Lake." *Science of the Total Environment* 752: 141966. https://doi.org/10.1016/j.scitotenv.2020.141966.

Clark, M. G., E. Humphreys, and S. K. Carey. 2019. "The Initial Three Years of Carbon Dioxide Exchange Between the Atmosphere and a Reclaimed Oil Sand Wetland." *Ecological Engineering* 135: 116–126. https://doi.org/10.1016/j.ecoleng.2019.05.016.

Clark, M. G., R. M. Petrone, and S. K. Carey. 2022. "Upland Reclamation Promotes Forest Evaporative Losses in the Boreal Plains of Canada: A Comparison of Carbon and Water Fluxes." *Agricultural and Forest Meteorology* 325: 109127. https://doi.org/10.1016/j.agrformet.2022.109127.

ClimateData.ca. 2025. Annual Values for Fort McMurray. https://climatedata.ca/explore/location/?loc=IAFFI&location-select-temperature=tx_max&location-select-precipitation=r1mm&location-select-other=frost_days.

Daly, C., J. Price, F. Rezanezhad, R. Pouliot, L. Rochefort, and M. D. Graf. 2012. "Initiatives in Oil Sand Reclamation: Considerations for Building a Fen Peatland in a Post-Mined Oil Sands Landscape." In *Restoration and Reclamation of Boreal Ecosystems*. Cambridge University Press. https://doi.org/10.1017/CBO9781139059152.012.

Devito, K., C. Mendoza, and C. Qualizza. 2012. *Conceptualizing Water Movement in the Boreal Plains. Implications for Watershed Reconstruction*. Canadian Oil Sands Network for Research and Development, Environmental and Reclamation Research Group.

Eaton, A. K., and W. R. Rouse. 2001. "Controls on Evapotranspiration at a Subarctic Sedge Fen." *Hydrological Processes* 15, no. 18: 3423–3431. https://doi.org/10.1002/hyp.1029.

Faubert, J. R., and S. K. Carey. 2014. "Growing Season Water Balance of Wetland Reclamation Test Cells, Fort McMurray, Alberta." *Hydrological Processes* 28, no. 14: 4363–4376. https://doi.org/10.1002/hyp.10240.

Gao, R., A. F. Torres-Rua, H. Nieto, et al. 2023. "ET Partitioning Assessment Using the TSEB Model and sUAS Information Across California Central Valley Vineyards." *Remote Sensing* 15, no. 3: 756. https://doi.org/10.3390/rs15030756.

Gavilán, P., J. Berengena, and R. G. Allen. 2007. "Measuring Versus Estimating Net Radiation and Soil Heat Flux: Impact on Penman–Monteith Reference ET Estimates in Semiarid Regions." *Agricultural Water Management* 89, no. 3: 275–286. https://doi.org/10.1016/j.agwat.2007.01.014.

Goulden, M. L., M. Litvak, and S. D. Miller. 2007. "Factors That Control Typha Marsh Evapotranspiration." *Aquatic Botany* 86, no. 2: 97–106. https://doi.org/10.1016/j.aquabot.2006.09.005.

Graham, A., B. Mudrzynski, E. Polzer, and D. A. Wilcox. 2022. "Restoration of a Lake Ontario-Connected Fen Through Invasive Typha Removal." *Restoration Ecology* 30, no. 4: e13562. https://doi.org/10.1111/rec.13562.

Harder, P., and J. W. Pomeroy. 2013. "Estimating Precipitation Phase Using a Psychrometric Energy Balance Method." *Hydrological Processes* 27, no. 13: 1901–1914. https://doi.org/10.1002/hyp.9799.

Haynes, W. 2013. "Wilcoxon Rank Sum Test." In *Encyclopedia of Systems Biology*, edited by W. Dubitzky, O. Wolkenhauer, K. H. Cho, and H. Yokota. Springer. https://doi.org/10.1007/978-1-4419-9863-7_1185.

Helbig, M., J. M. Waddington, P. Alekseychik, et al. 2020. "Increasing Contribution of Peatlands to Boreal Evapotranspiration in a Warming Climate." *Nature Climate Change* 10, no. 6: 555–560. https://doi.org/10.1038/s41558-020-0763-7.

House, M., D. H. Vitt, L. C. Glaeser, and J. A. Hartsock. 2022. "Reclaiming Wetlands After Oil Sands Mining in Alberta, Canada: The Changing Vegetation Regime at an Experimental Wetland." *Land* 11, no. 6: 844. https://doi.org/10.3390/land11060844.

Hu, Z., G. Yu, Y. Zhou, et al. 2009. "Partitioning of Evapotranspiration and Its Controls in Four Grassland Ecosystems: Application of a Two-Source Model." *Agricultural and Forest Meteorology* 149, no. 9: 1410–1420. https://doi.org/10.1016/j.agrformet.2009.03.014.

Huang, M., J. N. Hilderman, and L. Barbour. 2015. "Transport of Stable Isotopes of Water and Sulphate Within Reclaimed Oil Sands Saline–Sodic Mine Overburden." *Journal of Hydrology* 529: 1550–1561. https://doi.org/10.1016/j.jhydrol.2015.08.028.

Humphreys, E. R., P. M. Lafleur, L. B. Flanagan, et al. 2006. "Summer Carbon Dioxide and Water Vapor Fluxes Across a Range of Northern Peatlands." *Journal of Geophysical Research: Biogeosciences* 111, no. G4: G04011. https://doi.org/10.1029/2005JG000111.

Ireson, A. M., A. G. Barr, J. F. Johnstone, et al. 2015. "The Changing Water Cycle: The Boreal Plains Ecozone of Western Canada." *Wiley Interdisciplinary Reviews Water* 2, no. 5: 505–521. https://doi.org/10.1002/wat2.1098.

Jarvis, P. G., and K. G. McNaughton. 1986. "Stomatal Control of Transpiration: Scaling Up From Leaf to Region." *Advances in Ecological Research* 15: 1–49.

Johnson, J. W. 2000. "A Heuristic Method for Estimating the Relative Weight of Predictor Variables in Multiple Regression." *Multivariate Behavioral Research* 35, no. 1: 1–19. https://doi.org/10.1207/S15327906MBR3501_1.

Kelvin, J., M. C. Acreman, R. J. Harding, and T. M. Hess. 2017. "Micro-Climate Influence on Reference Evapotranspiration Estimates in Wetlands." *Hydrological Sciences Journal* 62, no. 3: 378–388. https://doi.org/10.1080/02626667.2015.1117089.

Ketcheson, S. J., J. S. Price, S. K. Carey, R. M. Petrone, C. A. Mendoza, and K. J. Devito. 2016. "Constructing Fen Peatlands in Post-Mining Oil Sands Landscapes: Challenges and Opportunities From a Hydrological Perspective." *Earth-Science Reviews* 161: 130–139. https://doi.org/10.1016/j.earscirev.2016.08.007.

Ketcheson, S. J., J. S. Price, O. Sutton, G. Sutherland, E. Kessel, and R. M. Petrone. 2017. "The Hydrological Functioning of a Constructed Fen Wetland Watershed." *Science of the Total Environment* 603: 593–605. https://doi.org/10.1016/j.scitotenv.2017.06.101.

Kljun, N., P. Calanca, M. W. Rotach, and H. P. Schmid. 2015. "A Simple Two-Dimensional Parameterisation for Flux Footprint Prediction (FFP)." *Geoscientific Model Development* 8, no. 11: 3695–3713. https://doi.org/10.5194/gmd-8-3695-2015.

Kruskal, W. H., and W. A. Wallis. 1952. "Use of Ranks in One-Criterion Variance Analysis." *Journal of the American Statistical Association* 47, no. 260: 583–621. https://doi.org/10.1080/01621459.1952.10483441.

Kurbatova, J., A. Arneth, N. N. Vygodskaya, et al. 2002. "Comparative Ecosystem–Atmosphere Exchange of Energy and Mass in a European Russian and a Central Siberian Bog I. Interseasonal and Interannual Variability of Energy and Latent Heat Fluxes During the Snowfree

Period." *Tellus Series B: Chemical and Physical Meteorology* 54, no. 5: 497–513. https://doi.org/10.1034/j.1600-0889.2002.01354.x.

Lafleur, P. M., R. A. Hember, S. W. Admiral, and N. T. Roulet. 2005. "Annual and Seasonal Variability in Evapotranspiration and Water Table at a Shrub-Covered Bog in Southern Ontario, Canada." *Hydrological Processes* 19, no. 18: 3533–3550. https://doi.org/10.1002/hyp.5842.

Lafleur, P. M., J. H. McCaughey, D. W. Joiner, P. A. Bartlett, and D. E. Jelinski. 1997. "Seasonal Trends in Energy, Water, and Carbon Dioxide Fluxes at a Northern Boreal Wetland." *Journal of Geophysical Research* 102, no. D24: 29009–29020. https://doi.org/10.1029/96JD03326.

Liljedahl, A. K., L. D. Hinzman, Y. Harazono, et al. 2011. "Nonlinear Controls on Evapotranspiration in Arctic Coastal Wetlands." *Biogeosciences* 8, no. 11: 3375–3389. https://doi.org/10.5194/bg-8-3375-2011.

Lu, L., D. Zhang, J. Zhang, et al. 2023. "Ecosystem Evapotranspiration Partitioning and Its Spatial–Temporal Variation Based on Eddy Covariance Observation and Machine Learning Method." *Remote Sensing* 15, no. 19: 4831. https://doi.org/10.3390/rs15194831.

Macdonald, E., S. Quideau, and S. Landhäusser. 2012. "Rebuilding Boreal Forest Ecosystems After Industrial Disturbance." In *Restoration and Reclamation of Boreal Ecosystems*. Cambridge University Press. https://doi.org/10.1017/CBO9781139059152.010.

Mauder, M., M. Cuntz, C. Drüe, et al. 2013. "A Strategy for Quality and Uncertainty Assessment of Long-Term Eddy-Covariance Measurements." *Agricultural and Forest Meteorology* 169: 122–135. https://doi.org/10.1016/j.agrformet.2012.09.006.

Mollard, F. P. O., M.-C. Roy, and A. L. Foote. 2013. "*Typha latifolia* Plant Performance and Stand Biomass in Wetlands Affected by Surface Oil Sands Mining." *Ecological Engineering* 58: 26–34. https://doi.org/10.1016/j.ecoleng.2013.06.017.

Moncrieff, J., R. Clement, J. Finnigan, and T. Meyers. 2005. "Averaging, Detrending, and Filtering of Eddy Covariance Time Series." In *Handbook of Micrometeorology*, 7–31. Springer Netherlands. https://doi.org/10.1007/1-4020-2265-4_2.

Moore, P. A., T. G. Pypker, and J. M. Waddington. 2013. "Effect of Long-Term Water Table Manipulation on Peatland Evapotranspiration." *Agricultural and Forest Meteorology* 178: 106–119. https://doi.org/10.1016/j.agrformet.2013.04.013.

Morison, M. Q., R. M. Petrone, S. L. Wilkinson, A. Green, and J. M. Waddington. 2020. "Ecosystem Scale Evapotranspiration and CO_2 Exchange in Burned and Unburned Peatlands: Implications for the Ecohydrological Resilience of Carbon Stocks to Wildfire." *Ecohydrology* 13, no. 2: e2189. https://doi.org/10.1002/eco.2189.

Nicholls, E. M., S. K. Carey, E. R. Humphreys, M. G. Clark, and G. B. Drewitt. 2016. "Multi-Year Water Balance Assessment of a Newly Constructed Wetland, Fort McMurray, Alberta." *Hydrological Processes* 30, no. 16: 2739–2753. https://doi.org/10.1002/hyp.10881.

Nicholls, E. M., M. G. Clark, and S. K. Carey. 2023. "Transpiration and Evaporative Partitioning at a Boreal Forest and Shrub Taiga Site in a Subarctic Alpine Catchment, Yukon Territory, Canada." *Hydrological Processes* 37, no. 6: e14900. https://doi.org/10.1002/hyp.14900.

Nichols, D. S., and J. M. Brown. 1980. "Evaporation From a Sphagnum Moss Surface." *Journal of Hydrology* 48, no. 3: 289–302. https://doi.org/10.1016/0022-1694(80)90121-3.

Nwaishi, F., R. M. Petrone, J. S. Price, and R. Andersen. 2015. "Towards Developing a Functional-Based Approach for Constructed Peatlands Evaluation in the Alberta Oil Sands Region, Canada." *Wetlands* 35, no. 2: 211–225. https://doi.org/10.1007/s13157-014-0623-1.

Oswald, C. J., and S. K. Carey. 2016. "Total and Methyl Mercury Concentrations in Sediment and Water of a Constructed Wetland in the Athabasca Oil Sands Region." *Environmental Pollution* 1987, no. 213: 628–637. https://doi.org/10.1016/j.envpol.2016.03.002.

Paul-Limoges, E., S. Wolf, F. D. Schneider, et al. 2020. "Partitioning Evapotranspiration With Concurrent Eddy Covariance Measurements in a Mixed Forest." *Agricultural and Forest Meteorology* 280: 107786. https://doi.org/10.1016/j.agrformet.2019.107786.

Peichl, M., J. Sagerfors, A. Lindroth, et al. 2013. "Energy Exchange and Water Budget Partitioning in a Boreal Minerogenic Mire." *Journal of Geophysical Research, Biogeosciences* 118, no. 1: 1–13. https://doi.org/10.1029/2012JG002073.

Petrone, R. M., U. Silins, and K. J. Devito. 2007. "Dynamics of Evapotranspiration From a Riparian Pond Complex in the Western Boreal Forest, Alberta, Canada." *Hydrological Processes* 21, no. 11: 1391–1401. https://doi.org/10.1002/hyp.6298.

Popović, N., R. M. Petrone, A. Green, M. Khomik, and J. S. Price. 2022. "A Temporal Snapshot of Ecosystem Functionality During the Initial Stages of Reclamation of an Upland-Fen Complex." *Journal of Hydrology: Regional Studies* 41: 101078. https://doi.org/10.1016/j.ejrh.2022.101078.

Popović, N., R. M. Petrone, A. Green, M. Khomik, and J. S. Price. 2023. "Evolution of Ecosystem-Scale Surface Energy Fluxes of a Newly Constructed Boreal Upland-Fen Watershed." *Ecological Engineering* 194: 107059. https://doi.org/10.1016/j.ecoleng.2023.107059.

Popović, N., R. M. Petrone, and J. S. Price. 2025. "Evapotranspiration Dynamics During the Ecosystem Development of a Constructed Upland-Fen Watershed." *Ecohydrology* 18, no. 2: e70022. https://doi.org/10.1002/eco.70022.

Price, J. S. 1994. "Evapotranspiration From a Lakeshore Typha Marsh on Lake Ontario." *Aquatic Botany* 48, no. 3: 261–272. https://doi.org/10.1016/0304-3770(94)90019-1.

Rooney, R. C., S. E. Bayley, and D. W. Schindler. 2012. "Oil Sands Mining and Reclamation Cause Massive Loss of Peatland and Stored Carbon." *Proceedings of the National Academy of Sciences of the United States of America* 109, no. 13: 4933–4937. https://doi.org/10.1073/pnas.1117693108.

Runkle, B. R. K., C. Wille, M. Gažovič, M. Wilmking, and L. Kutzbach. 2014. "The Surface Energy Balance and Its Drivers in a Boreal Peatland Fen of Northwestern Russia." *Journal of Hydrology* 511: 359–373. https://doi.org/10.1016/j.jhydrol.2014.01.056.

Scarlett, S. J., R. M. Petrone, and J. S. Price. 2017. "Controls on Plot-Scale Evapotranspiration From a Constructed Fen in the Athabasca Oil Sands Region, Alberta." *Ecological Engineering* 100: 199–210. https://doi.org/10.1016/j.ecoleng.2016.12.020.

Schulze, E.-D., R. Leuning, and F. M. Kelliher. 1995. "Environmental Regulation of Surface Conductance for Evaporation From Vegetation." *Vegetatio* 121, no. 1/2: 79–87. https://doi.org/10.1007/bf00044674.

Shveytser, V., P. C. Stoy, B. Butterworth, et al. 2024. "Evaporation and Transpiration From Multiple Proximal Forests and Wetlands." *Water Resources Research* 60, no. 1: e2022WR033757. https://doi.org/10.1029/2022WR033757.

Sonnentag, O., G. van der Kamp, A. G. Barr, and J. M. Chen. 2010. "On the Relationship Between Water Table Depth and Water Vapor and Carbon Dioxide Fluxes in a Minerotrophic Fen." *Global Change Biology* 16, no. 6: 1762–1776. https://doi.org/10.1111/j.1365-2486.2009.02032.x.

Spennato, H. M., S. J. Ketcheson, C. A. Mendoza, and S. K. Carey. 2018. "Water Table Dynamics in a Constructed Wetland, Fort McMurray, Alberta." *Hydrological Processes* 32, no. 26: 3824–3836. https://doi.org/10.1002/hyp.13308.

Strilesky, S. L., E. R. Humphreys, and S. K. Carey. 2017. "Forest Water Use in the Initial Stages of Reclamation in the Athabasca Oil Sands Region." *Hydrological Processes* 31, no. 15: 2781–2792. https://doi.org/10.1002/hyp.11220.

Thompson, C., C. A. Mendoza, and K. J. Devito. 2017. "Potential Influence of Climate Change on Ecosystems Within the Boreal Plains of

Alberta." *Hydrological Processes* 31, no. 11: 2110–2124. https://doi.org/10.1002/hyp.11183.

Tomlinson, S. A. 1996. *Comparison of Bowen-Ratio, Eddy-Correlation, and Weighing-Lysimeter Evapotranspiration for Two Sparse-Canopy Sites in Eastern Washington (No. 96-4081).* U.S. Dept. of the Interior, U.S. Geological Survey.

Tonidandel, S., and J. M. LeBreton. 2010. "Determining the Relative Importance of Predictors in Logistic Regression: An Extension of Relative Weight Analysis." *Organizational Research Methods* 13, no. 4: 767–781. https://doi.org/10.1177/1094428109341993.

Vickers, D., and L. Mahrt. 1997. "Quality Control and Flux Sampling Problems for Tower and Aircraft Data." *Journal of Atmospheric and Oceanic Technology* 14, no. 3: 512–526. https://doi.org/10.1175/1520-0426(1997)014<0512:qcafsp>2.0.co;2.

Vitt, D. H., L. C. Glaeser, M. House, and S. P. Kitchen. 2020. "Structural and Functional Responses of *Carex aquatilis* to Increasing Sodium Concentrations." *Wetlands Ecology and Management* 28, no. 5: 753–763. https://doi.org/10.1007/s11273-020-09746-9.

Vitt, D. H., M. House, and J. A. Hartsock. 2016. "Sandhill Fen, an Initial Trial for Wetland Species Assembly on In-Pit Substrates: Lessons After Three Years." *Botany* 94, no. 11: 1015–1025. https://doi.org/10.1139/cjb-2015-0262.

Vitt, D. H., R. K. Wieder, B. Xu, M. Kaskie, and S. Koropchak. 2011. "Peatland Establishment on Mineral Soils: Effects of Water Level, Amendments, and Species After Two Growing Seasons." *Ecological Engineering* 37, no. 2: 354–363. https://doi.org/10.1016/j.ecoleng.2010.11.029.

Volik, O., M. Elmes, R. Petrone, et al. 2020. "Wetlands in the Athabasca Oil Sands Region: The Nexus Between Wetland Hydrological Function and Resource Extraction." *Environmental Reviews* 28, no. 3: 246–261. https://doi.org/10.1139/er-2019-0040.

Volik, O., E. Kessel, A. Green, R. Petrone, and J. Price. 2021. "Growing Season Evapotranspiration in Boreal Fens in the Athabasca Oil Sands Region: Variability and Environmental Controls." *Hydrological Processes* 35, no. 2: e14020. https://doi.org/10.1002/hyp.14020.

Volik, O., R. Petrone, E. Kessel, A. Green, and J. Price. 2021. "Understanding the Peak Growing Season Ecosystem Water-Use Efficiency at Four Boreal Fens in the Athabasca Oil Sands Region." *Hydrological Processes* 35, no. 8: e14323. https://doi.org/10.1002/hyp.14323.

Volik, O., R. Petrone, and J. Price. 2024. "Wetlands as Integral Parts of Surface Water–Groundwater Interactions in the Athabasca Oil Sands Area: Review and Synthesis." *Environmental Reviews* 32, no. 2: 145–172. https://doi.org/10.1139/er-2023-0064.

Wang, X., Y. Zhou, H. Huang, et al. 2024. "Comparing Four Evapotranspiration Partitioning Methods From Eddy Covariance Considering Turbulent Mixing in a Poplar Plantation." *Water* 16, no. 11: 1548. https://doi.org/10.3390/w16111548.

Wardekker, J. A., D. Wildschut, S. Stemberger, and J. P. van der Sluijs. 2016. "Screening Regional Management Options for Their Impact on Climate Resilience: An Approach and Case Study in the Venen-Vechtstreek Wetlands in The Netherlands." *Springerplus* 5, no. 1: 750. https://doi.org/10.1186/s40064-016-2408-x.

Webster, K. L., F. D. Beall, I. F. Creed, and D. P. Kreutzweiser. 2015. "Impacts and Prognosis of Natural Resource Development on Water and Wetlands in Canada's Boreal Zone." *Environmental Reviews* 23, no. 1: 78–131. https://doi.org/10.1139/er-2014-0063.

Wu, J., L. Kutzbach, D. Jager, C. Wille, and M. Wilmking. 2010. "Evapotranspiration Dynamics in a Boreal Peatland and Its Impact on the Water and Energy Balance." *Journal of Geophysical Research: Biogeosciences* 115, no. G4: 2009JG001075. https://doi.org/10.1029/2009JG001075.

Wytrykush, C., D. H. Vitt, G. Mckenna, and R. Vassov. 2012. "Designing Landscapes to Support Peatland Development on Soft Tailings Deposits: Syncrude Canada Ltd.'s Sandhill Fen Research Watershed Initiative." In *Restoration and Reclamation of Boreal Ecosystems*. Cambridge University Press. https://doi.org/10.1017/CBO9781139059152.011.

Xu, Z., Z. Zhu, S. Liu, et al. 2021. "Evapotranspiration Partitioning for Multiple Ecosystems Within a Dryland Watershed: Seasonal Variations and Controlling Factors." *Journal of Hydrology* 598: 126483. https://doi.org/10.1016/j.jhydrol.2021.126483.

Zahn, E., and E. Bou-Zeid. 2024. "Observational Partitioning of Water and CO2 Fluxes at National Ecological Observatory Network (NEON) Sites: A 5-Year Dataset of Soil and Plant Components for Spatial and Temporal Analysis." *Earth System Science Data* 16, no. 12: 5603–5624. https://doi.org/10.5194/essd-16-5603-2024.

Zahn, E., E. Bou-Zeid, S. P. Good, et al. 2022. "Direct Partitioning of Eddy-Covariance Water and Carbon Dioxide Fluxes Into Ground and Plant Components." *Agricultural and Forest Meteorology* 315: 108790. https://doi.org/10.1016/j.agrformet.2021.108790.

Zahn, E., K. Ghannam, M. Chamecki, et al. 2024. "Numerical Investigation of Observational Flux Partitioning Methods for Water Vapor and Carbon Dioxide." *Journal of Geophysical Research: Biogeosciences* 129, no. 6: e2024JG008025. https://doi.org/10.1029/2024JG008025.

Zotarelli, L., M. D. Dukes, C. C. Romero, K. W. Migliaccio, and K. T. Morgan. 2010. *Step by Step Calculation of the Penman-Monteith Evapotranspiration (FAO-56 Method).* Vol. 8. Institute of Food and Agricultural Sciences. University of Florida.

Supporting Information

Additional supporting information can be found online in the Supporting Information section. **Data S1:** Supporting Information.